Chemical Papers (2024) 78:71–91
https://doi.org/10.1007/s11696-023-03089-4

REVIEW

A review on coatings through thermal spraying

Danial Qadir[1] · Rabia Sharif[2] · Rizwan Nasir[3] · Ali Awad[4] · Hafiz Abdul Mannan[5]

Received: 26 April 2023 / Accepted: 13 September 2023 / Published online: 30 September 2023

Abstract

Ceramic-coated metals with enhanced properties such as chemical and environmental deterioration resistance and high thermal stability have previously found widespread uses in various industries. However, their application was limited due to weak bonding at the interfaces of dissimilar materials. To achieve the necessary interfaces and bonding qualities, a variety of procedures, primarily mechanical treatments, were used. Interface structure and composition, transition temperature, and wettability are important characteristics. In this review, extensive study has been carried out for several thermal spray methods, such as flame spray, electric arc spray, and plasma spray technology. The study explores microstructural elements of plasma-sprayed coatings, including bonding mechanisms, pore creation, oxides formation, and other important process parameters. The study emphasizes how crucial wetness is to coating development. It looks at what affects wetting, how interfacial reactions affect reactive wetting, and how important additives or reactive materials are to encouraging wetting. In conclusion, the authors suggest the next studies and technological developments in coating technologies and thermal spray procedures. The study contributes to the continuous advancement of these processes and their applications by pointing out opportunities for more research and development.

Keywords Thermal spray coating · Wetting · Ceramic metal interfaces · Splat formation · Plasma-sprayed coatings

Introduction

In recent years, industrial growth has made it challenging to develop coatings with specific characteristics suitable for diverse operating conditions (Saleh et al. 2020; Deng et al. 2019; Ghanavati et al. 2021). The engineering materials deteriorate during services due to chemical, electrical, friction, electrochemical, and thermal reactions (Taleghani et al. 2021; Sopronyi et al. 2021). However, this deterioration can be handled effectively if the tribological and corrosion phenomena are adequately controlled (Jia et al. 2022; Hu et al. 2020). To impede or restrict the damage, selecting appropriate materials or surface coating technologies can be helpful (Donaldson 2021; Tscheliessnig et al. 2012; Winkless 2015).

A diffusion coating process is commonly defined as any process in which a base metal or alloy is either (i) coated with another metal or alloy and heated to a suitable temperature in a suitable environment or (ii) exposed to a gaseous or liquid medium containing the other metal or alloy, resulting in diffusion of the other metal or alloy into the base metal and changes in the composition and properties of its surface (Davis 2001). According to the literature, diffusion coatings can combine high hardness and good corrosion and wear resistance. Many coating technologies, including single and combination procedures, have been developed to create diffusion coatings. It has been revealed that, among other processing factors, treatment temperature has a significant impact on the resulting microstructures and diffusion coating qualities. Lower-temperature diffusion coating treatment produces continuous intermetallic compound layers based on the reaction–diffusion process. However, the eutectic reaction at higher temperatures results in a two-phase structure.

✉ Danial Qadir
D.Qadir@tees.ac.uk

1 School of Computing, Engineering and Digital Technologies, Teesside University, Middlesbrough TS1 3BX, UK

2 Department of Chemical and Polymer Engineering, University of Engineering and Technology Lahore (Faisalabad Campus), Faisalabad, Pakistan

3 Department of Chemical Engineering, University of Jeddah, Asfan Road, 23890 Jeddah, Saudi Arabia

4 Department of Chemical Engineering, University Teknologi PETRONAS, 32610 Sri Iskandar, Perak, Malaysia

5 Institute of Polymer and Textile Engineering, University of the Punjab, Lahore, Pakistan

As a result, the corrosion property of coatings, particularly their passivation behavior, is highly reliant on the production parameters, microstructure, and composition. Because of the uniform distribution of the passivating element, electrochemical experiments show that the continuous intermetallic compound layers display passive behavior (Zhong et al. 2012). Meißner et al. investigated three diffusion coatings (Cr, Ni + Cr, and Ni–P + Cr) on ferritic–martensitic X20CrMoV12-1 steel in a biomass-co-firing atmosphere. Exposures were conducted at 650 °C for up to 300 h with pure sulfates and a mixture of sulfates and KCl. Beneath the deposit of Na_2SO_4–K_2SO_4, the coatings proved to be highly resistant, whereas the addition of KCl drastically accelerated the corrosive attack (Meißner et al. 2020).

Surface coating technology most efficiently enhances hardness, atmospheric inertness, wear performance, corrosion, and erosion resistance without affecting the material's inherent properties (Banthia et al. 2020; Cui et al. 2021; Stathopoulos et al. 2016; Grammes et al. 2021). Surface coating allows bulk materials to remain intact, while surface functioning is designed to provide a more desired attribute. Ceramic coatings are ideal because they greatly improve metal surface qualities such as antifouling, self-cleaning, corrosion resistance, wear resistance, oil/water separation, and biocompatibility. Furthermore, numerous processes have been employed to create ceramic coatings with more desirable qualities on metal components, allowing the materials to be widely used in service environments (Dongmian and Xiaowei 2020). According to their chemical compositions, ceramic materials can be categorized as oxide and non-oxide. Numerous oxide ceramics are metal oxides that generate oxide films on their surfaces. They are utilized as coating materials to provide metallic materials with a protective and functional layer (for example, aluminum, stainless steel, or titanium alloys) (Dongmian and Xiaowei 2020). The metallic material is irreplaceable in industrial applications. The ceramic coatings bestow numerous unusual properties to metallic materials. Early in 1987, ceramic coating as thermal barrier coating was tested on turbine blades in a research engine. Today, thermal barrier ceramic coatings are used in a low-risk location within the turbine section of certain gas turbine engines (Miller 1987).

Functionally graded coatings are a new category of homogenous coatings having heterogeneous structures (Fathi et al. 2020) and are the combination of two or more phases to eradicate the residual thermal stresses (Rao et al. 2020; Amado et al. 2012). Functionally graded coatings (FGCs) can be produced by many manufacturing processes in recent years, including physical vapor deposition (PVD), thermal spraying, solution-state methods, chemical vapor deposition (CVD), induction heat treatment methods, and solution-state methods. However, each method has its advantages and drawbacks in its respective fields. The most challenging for each manufacturing method is to remove the residual and thermal stresses in the homogeneous coatings (Saleh and Ahmed 2021; Tyagi et al. 2019a).

Most engineering applications, such as aerospace, biomedical, vehicle, and environmental protection, require specific characteristics and features on the material surface (Liang et al. 2019). FGCs are coatings on the substrate having different compositions, thicknesses, microstructures, and gradient properties (Baghal et al. 2012; Ghadami et al. 2020). These graded coatings are in the most significant demand for their use in high-temperature applications involving energy generation, conversion, and utilization (Tsukamoto 2010). Moreover, preceding literature surveys depict the efficiency of FGCs in forming thermal barrier coatings, thermoelectric energy conversion products, corrosion-resistant coatings, and biomaterials (Moskal et al. 2019; Petrova and Schmauder 2020; Wang et al. 2022; Deng et al. 2021). The major thermal spraying techniques are air or vacuum plasma spraying (APS, VPS) by direct current (D.C.), radio frequency (R.F.) discharge-generated plasma, plasma transferred arc (PTA), wire (electric) arc spraying, flame spraying, high-velocity oxy-fuel (HVOF), high-velocity air fuel (HVAF), denotation gun (D-gun), and cold gas dynamic spraying (CS) (Galedari et al. 2019; Davis 2004).

In this paper, authors aim to review the present knowledge in the field of thermal spraying. This paper at first presents an overview of thermal spraying technologies and the latest developments in the area and then offers a detailed investigation of all the important phenomena (such as interfacial product formation, wetting, and splat formation) involved in these processes. Finally, they have provided readers with the issues and challenges presently faced by researchers in the aforementioned area. The authors believe this manuscript would be a valuable addition to the existing knowledge in this field for its detailed discussion and identification of challenges for future researchers.

Thermal spray processes

In this process, a target chemical metallic or nonmetallic material is sprayed upon a targeted surface (Vignesh et al. 2017; Pandey et al. 2018). The flame-accelerated molten or semi-molten feedstock material is sprinkled onto the substrate, usually in a wire, powder, or solution/suspension. Figure 1 shows a schematic representation. When fully or partially melted particles collide with the substrate, they deform and form splats. Mechanical impact followed by solidification causes the interlinkage of coated material with the substrate. Thermal spray techniques allow a wide range of materials to be deposited and worn sections quickly recoated (Davis 2004; Pandey et al. 2017; Tyagi et al. 2019b). Max Ulrich Schoop, a Swiss researcher,

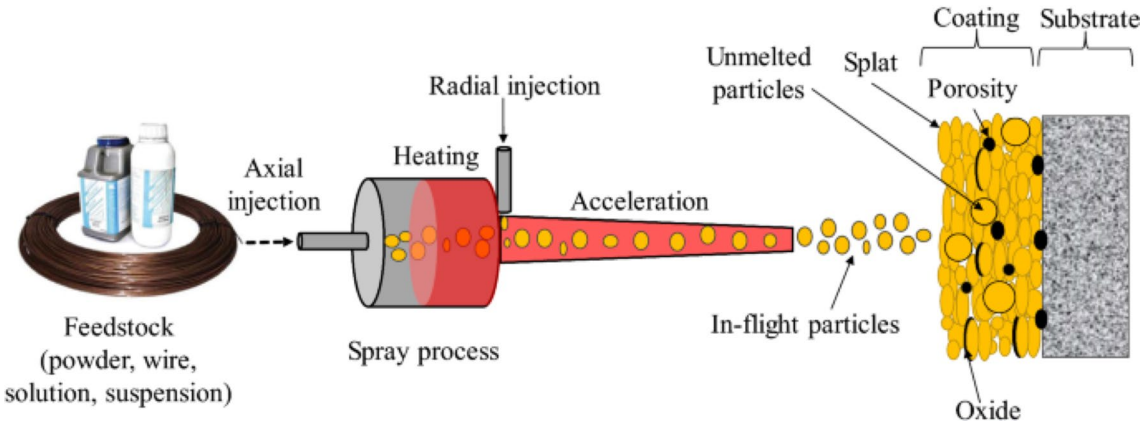

Fig. 1 Schematic illustration of thermal spray process adapted from Sadeghi et al. (2019)

published various patents (1882–1889) that contain the earliest information about thermal spraying with a modified oxyacetylene welding torch. Later, these torches were altered to utilize powder as a fuel source (Sadeghi et al. 2019).

The thermal spray technique was used in different countries, including Germany, the USA, and Russia, and used in various applications. Wire and powder flame spraying was the basis for the thermal spray method from the start of the 1920s to the 1950s. Fauchais et al. (2010) sprayed metal powders on the substrate using rocket engine technologies in the early 1980s, called high-velocity oxy-fuel spraying (HVOF). Browning (1992) pioneered the invention of high-velocity air fuel (HVAF) spraying, which includes the concept of "hypervelocity impact fusion." The powder material is injected into a convergent nozzle and carried by a hot supersonic gas stream at the temperature below the melting point of the feed stock powder, according to the original HVAF principle. De Laval nozzle is used to accelerate heated solid powder to extraordinary velocities. The kinetic energy of the particles is converted to thermal energy upon interaction with the substrate, which further warms the particles and melts them significantly to form a part of the coating (Kiilakoski et al. 2019; Murray et al. 2018).

The thermal spray processes are generally categorized by energy source type, shown in Fig. 2. The processes are classified based on the temperature and velocity of the jet stream produced. Splats are common in thermally sprayed coatings, but the nature of splat borders (commonly oxides at such boundaries), porosity, and residual stress vary greatly. Furthermore, corrosive chemicals can use the interplat bonding and linked pores as short-circuit diffusion pathways (Song et al. 2017). As a result, the microstructure and composition of coating material must be customized to assure their suitability in different applications, such as excellent corrosion resistance in hostile environments.

Flame spray process

Flame spraying is a century-old procedure that injects oxygen and fuel (acetylene or propane) through a gun nozzle, as shown in Fig. 3 (Xanthopoulou et al. 2014). Combustion of the gaseous mixture takes place before the nozzle forms a flame. The flame temperature varies between 3000 and 3300 °C depending on the oxygen-to-fuel ratio. The feedstock materials utilized can be in powder or wire form. Nickel- and cobalt-based alloys, some refractory metals, ZrO_2, Al_2O_3, TiO_2, and Cr_2C_3 in a NiCr matrix are some materials deposited using this process. The spray process is adaptable, portable, and has a low capital cost. Coatings with a high porosity content are frequently created using this approach (Singh et al. 2018).

The flame spraying process consumes less energy and is more cost-effective than any other thermal spray process; nevertheless, it lacks corrosion resistance. Rana et al. (2015) used a flame spray process to deposit NiCrAlY coatings exposed to atmospheric air and a solution of $Na_2SO_4 + V_2O_5$ salt at a temperature of 900 °C. The as-sprayed coatings had a unique morphology, including pre-oxidized alumina and unoxidized Ni and Cr regions. This shape protects against air oxidation and aids in confronting the harsh molten salt. The formation of nickel, chromium, and spinel oxides was developed all over the surface of a molten salt environment.

On the other hand, the pre-oxidized portion was unaffected by air oxidation. The porosity of the finishes had a minor impact on the oxidation of the air. High levels of in situ oxides and pores in flame-sprayed coatings hinder the process's effectiveness in general high-temperature applications.

Electric arc spray (wire arc) process

In the wire arc process, instead of using flame, twin consumable electrode wires were used to produce an electric

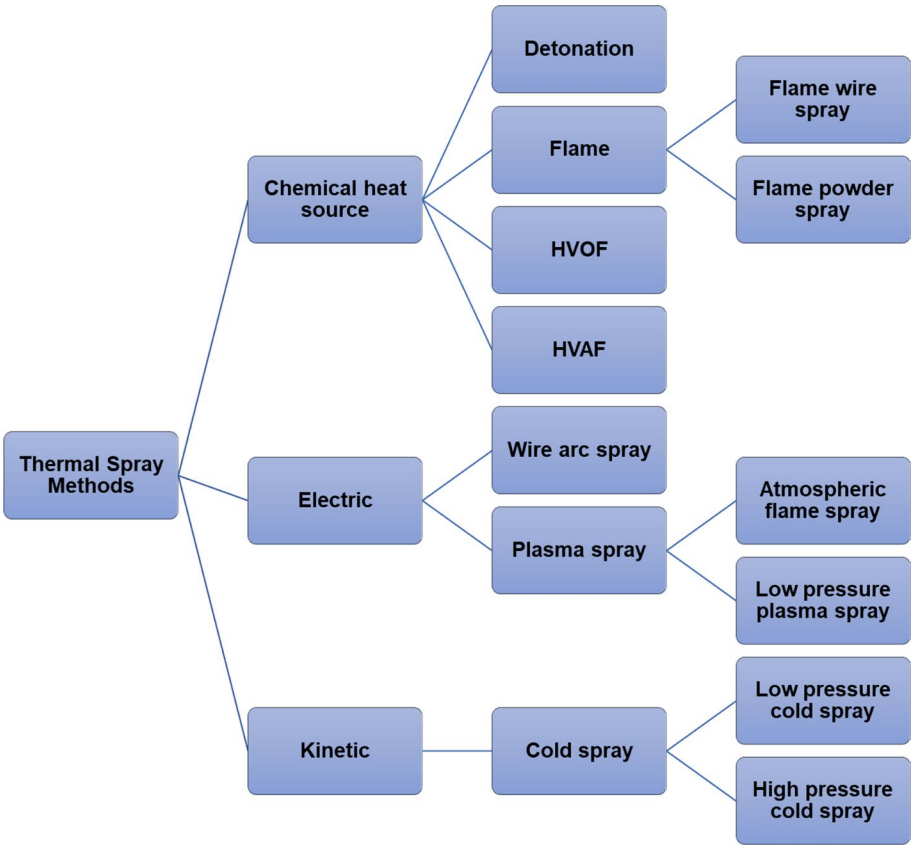

Fig. 2 Classification of thermal spray process adapted from Ann Gan and Berndt (2015)

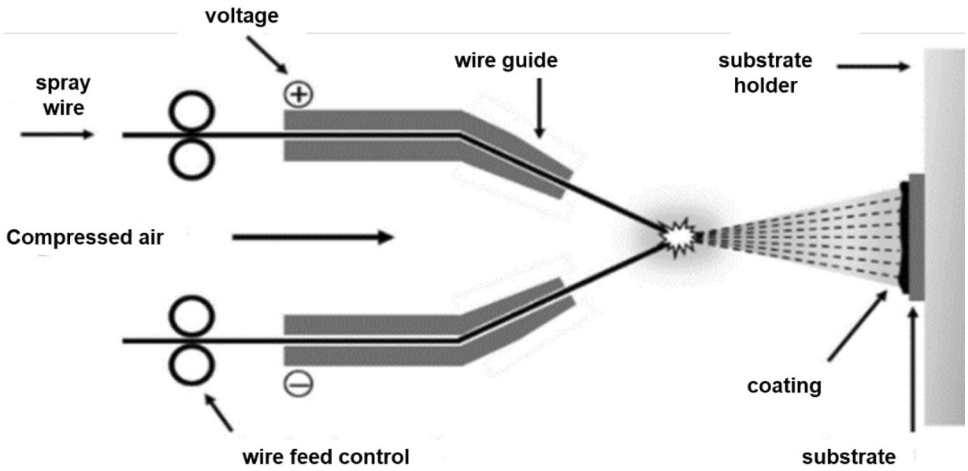

Fig. 3 Schematic diagram of the twin wire arc spraying process (Wagner 2021)

arc (controlled) to fuse the material to be coated. The wires contain chemical compositions like those of the required coating. The arc melts the wire from its tip. The molten material is crumbled and pushed toward the substrate surface by compressed air or inert gas jet. A diagram of the wire arc spraying technique is shown in Fig. 3. This process enhances bonding strengths and higher spray rates than the flame spray technique, but reduces porosities. Moreover, this process adversely affects humans and ecology, generating arc light, ozone, and fumes (Wagner 2021).

At 550 °C, an arc spray Alloy 625 coating was subject to atmospheric air for 168 h while exposing it to a KCl salt build-up was studied by Fantozzi et al. (2017). During the spraying process, the coating worked well as a higher degree of particle melting was useful in lowering interconnected porosity and impeding chlorine penetration. Although the formation of dense, non-porous oxides at the splat boundaries may act as barriers, their impact on the coatings' corrosion resistance is unknown. The chemical compositions rather than the microstructures of FeCrAlBY, Fe-based

coatings with high concentration sprayed by this technique were also helpful in receding high-temperature corrosion (Korobov et al. 2016). Both arc and flame spray methods are economical in boiler applications, and in situ, oxides and pores formed in the finishes prevent them from being used in high-temperature applications.

Table 1 compares the various properties of these processes. The choice of an appropriate process is influenced by several factors, the most important of which are coating material, coating performance, and process cost (Herman et al. 2000). Various feedstock, including rods, wires, and powders, are used for coating and process needs. Typically, feedstock sizes are maintained within specified parameters, 5–100-micron-size powder. Spraying characteristics such as the particle's velocity, the powder's feed rate, the flame's temperature, and powder morphology, among others, must be combined to produce advantageous coatings. The oxide content, porosity, and bond strength of a coating can all be used to assess its quality. Depending on the various coating settings, the coatings thickness created by the above-mentioned techniques ranges from 2.5 mm to 25 microns (Talib et al. 2003).

Plasma spray technology

In APS, the feedstock material is sprayed with a plasma jet in air circumstances (Shin et al. 2017). The APS technique allows the spraying of nearly any feedstock material, including ceramics, as plasma has a high flame temperature (15,000 °C) and plasma jet has tremendous thermal energy (Fauchais 2004).

Sadeghimeresht et al. used APS to deposit three distinct Ni, Ni_5Al, and Ni21Cr coatings. This technique was deemed unsuitable for corrosion protection applications because of its high porosity and many unmelted particles (Sadeghimeresht et al. 2016). Hussain et al. investigated four different nickel- and iron-based alloy compositions (NiCr, Alloy 625, NiCrAlY, and FeCrAl) sprayed using the APS technique present in advanced fossil fuel facilities to address fireside corrosion involving coal/biomass-produced flue gases. This process occurred in a controlled condition for 1000 h at 650 °C in a furnace with a coal ash accumulation (Na_2SO_4, Fe_2O_3, and K_2SO_4). At the same time, the NiCr coating serves as superior to the other coatings (NiCr > FeCrAl > Alloy 625 > NiCrAlY), and all the finishes were subjected to severe corrosion. Because of the significant porosity and inadequate intersplat bonding, corrosion in the coatings progressed quickly (Hussain et al. 2013). Singh et al. looked at an APS NiCrAlY coating at 900 °C exposed to air under cyclic circumstances. (Each cycle consists of one hour of heating followed by cooling for 20 min.) The coating adhered well to the substrate surface and formed scales of oxide that guard it from oxidation; the porosity and inadequate intersplat bonding was cited as the main causes of coating failure (Singh et al. 2005).

In conclusion, functionally graded coatings represent a significant development in the advancement of thermal spray technology. These coatings effectively close the gap between coatings and substrates by enabling the seamless integration of various materials. Both conventional and modern methods are used in this evolutionary journey. While traditional methods use different injections or mixed powders to deposit multiple coatings, modern techniques embrace hybrid methodology. Various feedstocks, including powders, suspensions, and solutions, are used in these innovative techniques. These advances promise to change the face of surface engineering and material enhancement as the field of functionally graded coatings develops (Łatka et al. 2020).

Microstructure of plasma-sprayed coatings

The quantitative estimates of the lamellar interface bonding ratio help us understand how spray parameters affect the lamellar interface bonding. It also provides necessary data to develop relationships between the microstructure of coating and properties and the study of how and why spreading droplet bonds to the underlying splats. McPherson

Table 1 Thermal spray process properties (Herman et al. 2000)

Type of spray		Rate of gas flow (m^3/hr)	Temp. of flame (°C)	Particle's velocity (m/s)	Power (kW)	Spray distance (mm)	Microstructural features
Combustion (powder and wire)		11–71	3000	40–100	25–75 50–100	120–250	High porosity oxidation
HVOF		28–57	3000	400–800	100–270	150–300	High value of density Good adhesion property
Two wire Arc		71	3000–6000	50–150	4–6	50–170	Dense and good thickness
Plasma	APS	4.2	5000–25000	80–300	30–80	60–130	Porosity in ceramic deposits
	VPS	8.4		–	50–100	300–400	
Cold spray		60–120	Room temp.	400–800	5–25	10–50	Dense, compressive stresses

(McPherson and Shafer 1982) attempted the first quantitative estimation of the real contact ratio based on the relative Young's modulus of a plasma-sprayed ceramic coating concerning the comparable bulk.

Previous studies have examined the oxidation behavior of coatings applied using popular thermal spraying procedures, including APS and HVOF (Chatha et al. 2013; Oksa et al. 2015; López et al. 2014). Nevertheless, the coating characteristics linked with the preceding approaches, such as pores, splat boundaries, and in situ-produced oxides (Song et al. 2017), result in the production of a discontinuous oxide scale, prompting researchers to look for a more efficient protective resistor. The greater number of linked pores in the coatings and poor splat cohesion caused by oxides and voids generated at the splat boundaries have a negative impact on the coatings' oxidation behavior (Uusitalo et al. 2002).

Plasma spraying involves the application of a projection of semi-molten, molten, or unmolten particles incident on a target metal surface, which creates layer of coating on the surface. Due to non-equilibrium events during swift solidification, plasma spray provides a covering with a highly thin microstructure. Respective particles may touch the surface of the substrate or a pre-deposited layer when applying spray (Roche et al. 2022). After spraying, particles likely form a structure like pancake- or lamella-like layer structure on the substrate surface. Due to multiple elongated grains linked to one another, including internal fissures, pores, and unsoften particles, the pancake-like structure is heterogeneous. As a result, a good coating is usually thought to have a lamella-like homogenous structure with fine grains. The active sites offered by the pores and oxides are primarily responsible for the connection between these already deposited particles and the current sprayed particles. Certain parameters such as velocity, diameter, temperature, morphology, and pressure are critical considerations for the coating process. The substrate's surface roughness and the sprayed particle's solidification determine the molten particle's flattening. However, studies have concluded that managing parameters for successful coating include impinging droplet factors and substrate parameters and that a mix of both is sometimes required for quality coating (Dhiman et al. 2007). Figure 4 shows the thermally sprayed coating features, such as oxides, debris on the target surface, surface porosity, and semi-melted particles.

However, due to its extreme mechanical weakness, the resulting microstructure can be far more prone to delamination than its forerunners. Alternately, one may concentrate on improving the stoichiometry of the plasma-sprayed HA coatings. Still, with the necessary spraying conditions, it might be difficult to incorporate the type of microstructure required/porosity. In this light, layered "functional" osteoconductive coatings might be seen as a technique to advance

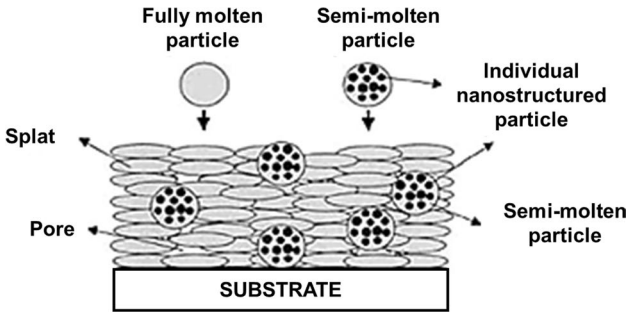

Fig. 4 Microstructure of the internals of thermal spray coating process (Fauchais et al. 2010; Lima and Marple 2007)

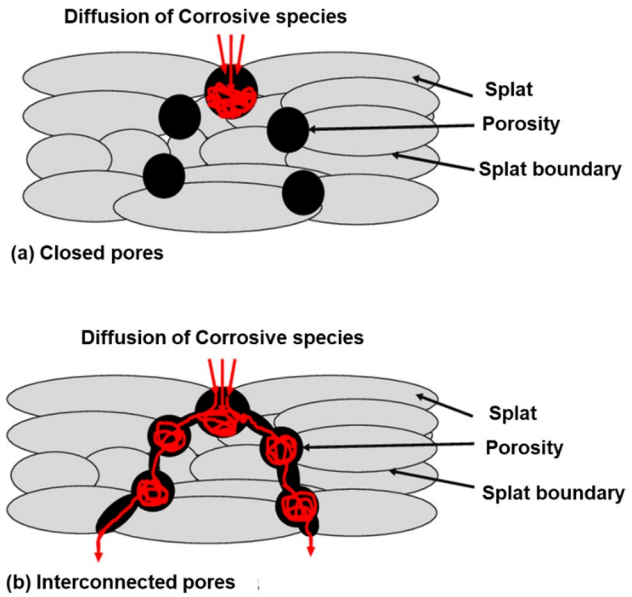

Fig. 5 Splat boundaries in the corrosion of coatings (Sadeghi et al. 2019; Sadeghimeresht 2018)

the state of the art of technology (Gildersleeve and Vaßen 2023).

Bonding mechanism

When hitting particles flatten out in spraying processes, they are called "splats," which might be disks, splashes, or fragmented splats. A thermally sprayed covering was formed when numerous overlapped splats hardened and attached, as shown in Fig. 5. As a result, a fundamental structural component of thermal spray coatings is a splat. When speeding particles collide with a surface, splats form. The approaching molten or semi-molten droplets are mostly spherical, flattening and dispersing in the shape of disklike formations (splats) to fill the underlying interstices upon collision with the substrate surface (free spaces).

Regardless of the thermal spray method, splats and splat boundaries are present in each thermal spray coating (Sadeghi et al. 2019). The distance between two splats indicates the particle melting in flight and the deformation caused by the hit (if the particle does not melt completely). As seen by these splats, the degree of melting notably affects the coating's adhesion, cohesion, porosity, and future corrosion properties (Fauchais et al. 2014).

In developing a coating, the shape of each splat is crucial. Disk splats are the most preferred among other splats because they are expected to adhere well to the outer surface of the substrate. Because it is established that the adhesive strength of any coating determines the quality, attaining disk splats in spraying becomes preferable (Zhang et al. 2016a). These incident particles may bond with the surface of the substrate in multiple ways, such as mechanical bonding, chemical bonding, or diffusion (Parmar et al. 2022). The bonding through diffusion is postulated to happen during high temperatures while spraying, and the surface of the substrate is clean from oxides. The bonding among splat atoms and substrate interface controls the mechanism. To establish diffusion bonding type in the process of spraying, the temperature of the substrate must be kept at a higher value while a layer of oxide is removed. Diffusion is usually accomplished with the use of a gentle vacuum. The impacting particle's velocity is higher enough to distort the oxide's layer on the substrate surface in cold spray procedures (Klinkov and Kosarev 2006). The process of chemical adhesion is aided by the incident particle's ability to melt the substrate's surface, which is usually observed when the impacting particle has a higher melting point than the substrate surface. It was also suggested that in the case of chemical adhesion, greater adhesion strength is related to the production of compounds at the splat–substrate interface (Harun et al. 2018; Morks et al. 2002; Chandra and Fauchais 2009). Munroe et al. also observed that when NiCr particles were thermally sprayed over an aluminum substrate, the substrate melted to a depth of several microns. This also revealed the existence of deformation of the substrate and Ni and Al interdiffusion throughout the contact (Brossard et al. 2010a).

Ahmad et al. studied the crystallization and adhesive properties of hydroxyapatite (HA) coating applied by chemical technique and sintering at 500, 600, and 700°C on an AISI 316L stainless steel substrate. The results show increased adhesive strength and a significant improvement in HA coating crystallization (Ahmed et al. 2015). Line et al. created hydrogen-induced graphene on an Ir surface; strong bonding was formed at the graphene–substrate contact, considerably improving carbon monoxide corrosion resistance (Kyhl et al. 2018).

On the other hand, mechanical adhesion is a deliberate effort, such as grit abrasive blasting, to improve adherence between sprayed particles and incident target surfaces. Splats often shrink as they cool, and by interlocking, they stick to the surface pits and grooves of the roughened substrate. Many types of research have shown that increased surface roughness can improve mechanical adhesion because it is thought that greater roughness creates more physically active bonding sites (Viscusi et al. 2019; Fauchais et al. 2004). Rath et al. (2012) formed the TiO_2/HAp bilayer coating that depicted a remarkable increase in the bonding strength (48 MPa) and corrosion resistance without disturbing its biocompatibility compared to monolithic coating. Mechanical interlocking and diffusion bonding at the contact were responsible for the significant rise in adhesion strength. Cedelle et al. claimed that heat treatment enhanced the segment of disk splats in the system, including Ni, Cu, and YSZ, on substrates of stainless steel material and YSZ-coated substrates. Heat treatment of the substrate significantly increased the skewness value, allowing the morphology of the splats to be modified to disk-shaped splats (Cedelle et al. 2006).

Pores

For most technical applications, porosity in plasma-sprayed coatings is critical. Porosity offers advantages and disadvantages depending on the coating's functionality and the immediate working environment. As a result, the porosity generation and development mechanisms have been intensively investigated to determine methods of controlling porosity in plasma-sprayed coatings (Odhiambo et al. 2019). Spray process factors influence porosity features such as morphology, pore diameters, pore distributions, microcrack sizes and orientations, and lamellar splats—furthermore, the type of components and bonding mechanisms impact pore distributions (Ctibor et al. 2006). Unmelted particles are the most typical source of coating porosity. The temperature of the arriving droplets can vary from perfectly molten liquid to a fully unmolten solid state, depending on the particle temperature. The droplets of liquid flow freely and cover most of the spaces. The impact velocity of solid or partially melted particles should be high enough to deform plastically upon impact. As a result, a particle having higher velocities results in greater particle deformation and, as a result, finer void closing. If the impact velocity is modest, the solid particles may become stuck in the coatings due to later approaching particles. These unformed particles are poorly bound and should further apart with the underlying splat, forming voids (Sadeghi et al. 2019).

Thermal spray coatings often avoid porosity because it lowers the coating's strength by generating delamination, cracking, or spallation. In certain circumstances, such as coatings of wear resistance, porosity is occasionally desirable to obtain coatings having lower-thermal-conductivity properties, as these pores are expected to form the insulation

for coating. Porosity can be regulated in either scenario, depending on the desired coating characteristics and the appropriate process conditions (Davis 2004).

It is generally known that the pore content of a coating has a significant effect on its corrosion resistance (Campo et al. 2009; Bolelli et al. 2008; Milanti et al. 2015; Zhang et al. 2016b). Corrosive species can easily invade porous coatings and approach the substrate if they are porous. The coating will delaminate early in such instances, and its ability to provide protection will be compromised. Through porosity (interconnected) and closed porosity are the two types of porosity, and each plays a different function in defining the corrosion behavior of the coatings. Interconnected porosity is considerably more susceptible to corrosion than closed porosity because it provides direct routes between the substrate and the corrosive environment (Arrabal et al. 2010).

The local chemistry of the coating is altered by porosity, which favors corrosion (Ctibor et al. 2006). The surface film in zones of higher porosity in a Fe49.7Cr18Mn1.9Mo7.4W1.6B15.2C3.8Si2.4 (at. percent) amorphous coating has a little bit higher concentration of Cr (3–4%); mainly concentration of Cr^{6+} dominates the concentration of Cr^{3+}, according to X-ray photoelectron spectroscopic analysis. The external layer of the passive film, which is often faultier, comprises this high-valence species. The uneven distribution of Cr on the coating surface lacks corrosion resistance due to high porosity, as shown in Fig. 6, which depicts corrosion damage induced due to high porosity on the coating surface.

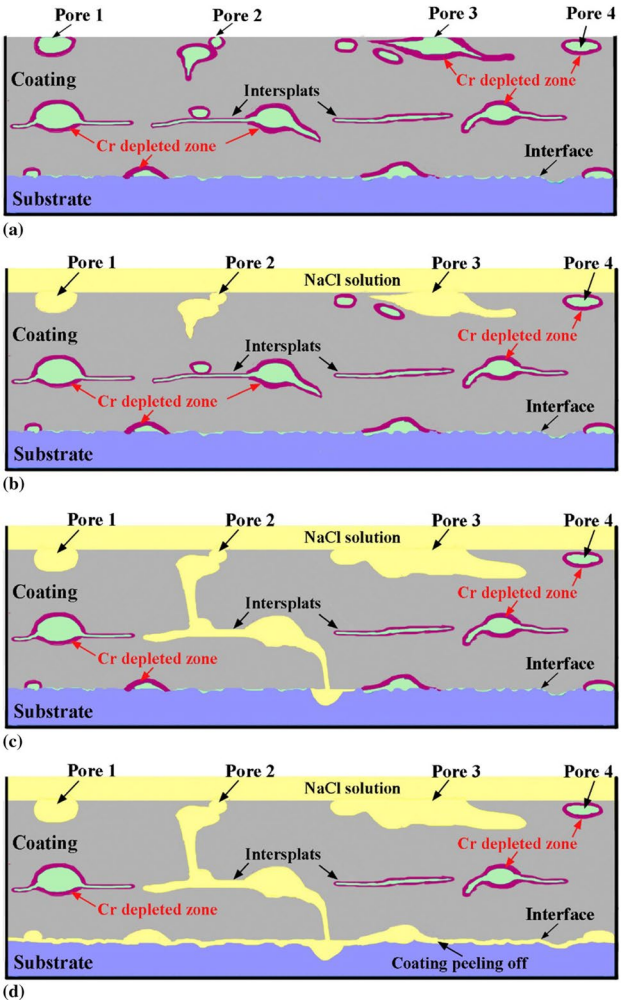

Fig. 6 Corrosion effects on the substrate surface coated with a Fe-based amorphous alloy adapted from Zhang et al. (2016b)

Oxides and phases

During spray processing, oxide layers form on reactive metals such as aluminum, nickel, chromium, and others, which have consequences for the microstructure and coatings bonding (Sun et al. 2019)(40). These oxide layers reduce the degree to which molten particles spread after effect on that substrate, increasing the coating porosity and acting as interfacial friction between the substrate and the splat (Fanicchia et al. 2018).

Brossard et al. confirmed the presence of oxides in the microstructure of plasma-sprayed NiCr. They observed the oxidation of metal particles while spraying in two forms, i.e., either in globular form (entrapped in droplet) or spinel (outer surface). Later, this oxidation process appears as a ringlike granular inside spray coating. It was also observed that high temperatures and low oxygen concentrations are to blame for the oxidation of some metals (Brossard et al. 2010b).

Grimm et al. investigate the microstructure and hardness of coatings made by atmospheric plasma spraying with a commercially available $(Al,Cr)_2O_3$ solid solution powder mixed with varying concentrations of TiO_2. According to the findings, coupling with TiO_2 reduces porosity and defect density while boosting deposition efficiency and microhardness. Coatings made from mixes with increased TiO_2 concentration had small quantities of Ti in solid solution $(Al, Cr)_2O_3$ splats. Aluminum and chromium concentration variations were also discovered (Grimm et al. 2021). Rezakhani (Rezakhani 2007) focuses on FeCrAl and Tafaloy 45CT (arc-sprayed) and 50Ni–50Cr and Cr_3C_2_NiCr (HVOF-sprayed) coatings when exposed to 550 and 650 °C for 8 days with a synthesized ash containing 70% of V_2O_5, 20% of Na_2SO_4, and 10% of NaCl.

Parameters

According to much research, coating formation is influenced by various factors, including spraying technique, spraying parameter, splat properties, and substrate materials. These settings are tuned to get the required coating quality. Critical characteristics include the temperature of the substrate, the morphology of the substrate, splat impact, cooling rate,

splat temperature, thermal contact resistance, spraying distance, and the angle at which the spray is done (Kadam et al. 2022b). Rousseau et al. (2021) found that combining a spray from a shorter distance with less power improved coating microstructure and characteristics. The effect of irregular, spherical, and nanostructured agglomerated powders on the porosity of coating and bonding strength was investigated by Shi et al. (2020). The porosity and binding strength of spherical and irregular powders were higher.

Zhang et al. (2019) studied the microstructure and mechanical properties of in-flight particles as a function of velocity and temperature. They discovered that partially melted particles in flight with high temperature and velocity cause themselves to become fully molten. Mihm et al., (2012) inquired about various nozzle designs, including standard cylindrical and vacuum monomer technique (VMT) nozzle, to enhance plasma spray's performance and deposition efficiency. Because it uses a single cathode–anode plasma gun, a typical cylindrical nozzle limited plasma flow control, he also indicated that a vital component in managing coat quality is the plasma gas to flow rate of carrier gas ratio for feeding powder. It was also observed that with the increase in plasma gas ratio, plasma jet temperature also increases, while an increase in carrier gas flow rate aids the powder's entry into the plasma jet's center. If the flow rate of carrier gas is very high, then the plasma jet will move out of its typical point, resulting in a non-uniform thickness of coating and less deposition efficiency.

Myoung et al. (2010) investigated the coating microstructure, which may be influenced by changes in the feeding powder and the use of numerous hopper systems. Bertrand et al. (2008) studied the influence of spray angle on the coating structure and characteristics. The spray angle affected deposition efficiency by influencing the powder sticking coefficient. Only a few cracks with a crack length of less than 30° result from a high spray angle, resulting in a better coating structure. Kadam et al. (2019, 2022a) probed the influence of spray angle on the coating structure and discovered that grain shape, size, and distribution all changed. The reduction in spray angle causes elongation in the grain size and shape. The spray angle parameter also impacts the porosity in the coating structure. Mantry et al. (2014) investigated the effects of various spraying parameters and discovered that the impact velocity angle and temperature are important determinants in coating performance. The influence of substrate rotation on the microstructural and mechanical properties of 8YSZ TBCs was studied by Kadam et al. (2020). They discovered that changing the porosity and hardness of the substrate impacts the coating structure. Garcia et al. (2008) looked at how the structure of pores and the orientation and structure of the splat layer affect microstructural features throughout the deposition process. They also looked at how the pores' structure (shape and size) and the orientation and splat layer structure affect the microstructural properties of the deposition process. Wang et al. (2018) investigated the effect of the spraying powder on the hardness, nanostructure, and level of porosity of coating.

Morphology of splats

Adhesion and cohesion are two types of bonding that occur during thermal spraying. According to the coating formation hypothesis, the basic ideas for developing thermal spray coating include quick radial expansion on the substrate surface, rapid cooling, and solidification upon impact of molten droplets. Individual splats are created due to these processes, and the sequential piling of splats forms the coating. As the individual splat formation proceeds, bonding takes place at the same time. As a result, studying splat formation is the first step toward determining what factors influence bonding formation kinetics (113).

The shape of the splat influences adhesion/cohesion. During splat creation, splashing is common, resulting in weakly adhering radial arms or tiny particles (Li et al. 2022). Over the last thirty years, intensive research has revealed that the temperature at which the substrate surface is preheated significantly influences splat shape (Yao et al. 2016; Li et al. 2013; Fukumoto et al. 2004; Li and Li 2004a), and splat–substrate thermal contact (McDonald et al. 2007a). Splats are deposited on a polished smooth substrate with adsorption of moisture contents or other adsorbates that evaporate in an ambient atmosphere; the resulting splats have irregular shapes that do not follow any rules, but are irregular at random (Moreau et al. 1995). Upon heating, the substrate surface eliminates any surface-adsorbed moisture, and a regular disk splat on a clean, uniform substrate is frequently obtained (Fukumoto et al. 2004; Li and Li 2004a). The disk splat represents splats arranged in disk shape with few radial arms. These criteria for the Reynolds numbers can be met for most ceramic spray materials (Goutier et al. 2013; Blanchi et al. 1995; Bhusal et al. 2019; Zhang et al. 2016a).

The size of a regular disk splat

The spray molten droplet parameters determine the size/diameter of typical disklike splats, such as size, velocity, temperature, and the thermal contact of the molten droplets with the substrate, resulting in a spreading restriction due to quick solidification. The flattening ratio, defined as the ratio of disk splat diameter (D) to the initial droplet diameter, determines the splat size *(d).* The Reynolds numbers of molten droplets (Re) can relate to the flattening ratio ($\mathcal{E}$) (Madejski 1976):

$$\varepsilon = a\mathrm{Re}^{b} \tag{1}$$

where a and b are constants with the values of 0.125 (Jones 1971) and 0.2 (Madejski 1976) obtained by theoretical

modeling. They can also be found by the regression of the data acquired by simulation, assuming $b = 0.2$ (Jones 1971; Li et al. 2005; Li and Li 2004b) or experiments with $b = 0.125$ (Li et al. 2005). The Reynolds number (Re) is expressed as:

$$\mathrm{Re} = \frac{\rho_p d_p V_p}{\mu_p} \tag{2}$$

where ρ_p, d_p, μ_p, and V_p are the density, diameter, viscosity, and velocity of particles, respectively. The temperature of the particle droplet determines all these parameters. The degree of flattening and particle size are the variables on which the diameter of a regular disk splat depends in the ideal scenario of generating a regular disk splat following a fused droplet impact on a substrate, as illustrated in the above equation. The flattening degree enhanced with particle velocity and temperature increases, and the splat thickness was reduced. At the same time, the experimental results affirmed that the degree of flattening of ceramic droplets ranges from 3 to 5 for ceramic spray materials and spray circumstances (Fauchais et al. 2010), corresponding to a splat thickness from 0.6 to 3.0 µm.

Cedelle et al. confirmed the impact splashing phenomenon by spraying partly stabilized yttria zirconia (8wt%) on a mirror-polished surface of stainless steel material. They analyzed that this phenomenon happened within a few hundred nanoseconds in the direction of impact or parallel to the surface of the substrate at an incident angle of less than 45°. Because of thermal flow instabilities caused by wave energy propagation at impact, splashing occurs at this early stage (within 100 ns) (Cedelle et al. 2005). Armster et al. proposed that the primary reason is compression wave for instability at droplet impact generated at impact time (Armster et al. 2002). Mundo et al. presented the splashing parameter Sommerfeld "K" that primarily depends on the Weber number and Reynolds number of impacting droplets. The relation is as follows.

$$K = \mathrm{We}^{0.5}\mathrm{Re}^{0.25} \tag{3}$$

where $We = \rho.D.v^2 / \sigma$ is the Weber number and $Re = \rho.D.v/\mu$ is the Reynolds number. It is projected that the value of $K < 3$ matches the rebounding of the splat, and a value higher than 57.7 depicts the splashy nature of splats. Furthermore, K's value ranges from 3.1 to 57.7, which is a reasonable value for splat deposits (Mundo et al. 1995). Dhiman et al. sprayed *Ti* droplets on several substrates and confirmed the above claim, concluding that the Sommerfeld parameter K values for thermal spraying may change depending on substrate circumstances. They measured K values for substrates kept at temperatures significantly higher than Mundo predicted for disk-shaped splats (Dhiman and Chandra 2005). Shiraz et al. investigated the effects of varying tin droplet impact velocities on a stainless steel substrate. They discovered that the striking droplet's velocity significantly impacts the droplet's final shape. They also concluded that the molten droplet's impact velocity decisively determines the droplet's spread factor *(ξ = D/Do)*. The fact given by Shiraz et al. is shown in Fig. 7 (Aziz and Chandra 2000).

Droplet flattening

The incident particle's features and the substrate material's properties influence the droplet's flattening. The characteristics like roughness, rate of solidification, materials' thermal diffusivities, contact quality, thickness alongside substrate oxide layer's roughness, condensates and additional adsorbates, temperature, and thermally contact resistance of substrate are only a few of the critical aspects that affect coating quality (Fauchais et al. 2004). According to Fukumoto et al., the flattening process of the droplet has a significant impact on the adhesion of a coating. Furthermore, he asserts that the governing parameters for the flattening mechanism include the particle's velocity, temperature, wetness at the splat interface, and substrate and substrate temperature. He established that even flattening in response to minimal roughness and preheating of substrate aids in creating disk-form splats in his research of hitting Ni particles on various substrates. He also claimed that "flattening splashing," or splashing that occurred during flattening (visually observed as the formation of a finger parallel to the surface of the substrate), can occur when solidification begins immediately after impingement or substrate roughness prevents the liquid droplet front from flowing smoothly on the substrate surface. He indicated that in a metal/metal combination, fast solidification is likely to be a key component in flattening splashing. Inada Young and Mostaghimi concurred that the hardened layer at the bottom of the splat could present problems during the flattening of the top molten regions (Fukumoto and Huang 1999).

Impact of substrate characteristics on droplet flattening

Several researchers looked at the importance of substrate morphology. They suggested that substrate surface conditions, such as adsorbates or condensates, roughness, and oxides, are important in achieving the required coating quality (Fauchais et al. 2004). Fujimoto et al. studied the substrate conditions and found that heat treatment improved roughness, which might influence the morphology of splat and surface roughness at the nanoscale, improving substrate wettability (Fujimoto et al. 2007). According to McDonald, the preheating of substrate metal changed the external composition by forming an additional layer of oxide, which enhanced the splat structure from splash to disk splats.

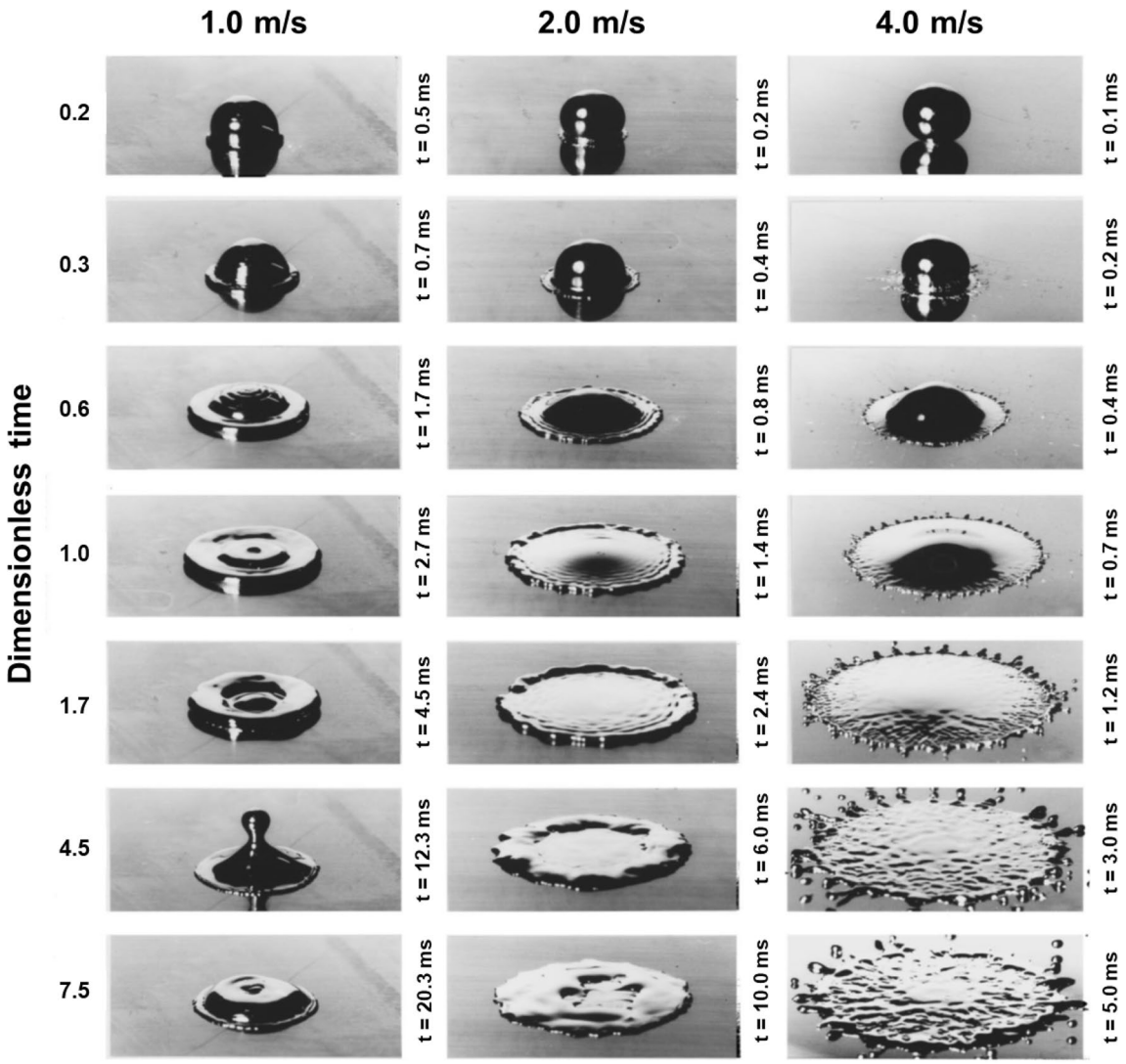

Fig. 7 Molten tin droplet impact on the surface of stainless steel (25 °C) with variable velocities adapted with permission from Aziz and Chandra (2000)

McDonald et al. further claimed that creating this oxide layer prevented re-adsorption on the substrate surface, which improved the splat shape (McDonald et al. 2007b). Jiang et al. observed that condensates/adsorbates play a vital role in particle flattening. They claimed that vaporization happens at the surface when a molten particle collides with a low-temperature substrate, promoting the creation of pores and voids. These condensates/adsorbates evaporate during heating on hot substrate surfaces, and the impacting incident particle attains a nice quality contact on this fresh surface (Jiang et al. 2001).

Brossard et al. confirmed that substrate roughness has a role in producing voids and oxides in the study. They also claimed that the roughness of a substrate could cause it to melt, creating voids and mixed oxides on the surface (Brossard et al. 2010c). Mc. Donald et al. researched the importance of resistance through thermal contact and found that setups with lower resistance through thermal contact had disk splat morphology. In comparison, systems with higher resistance through thermal contact had disk splat structures (McDonald et al. 2007a). Resistance through thermal contact depends not only on the substrate surface parameters but also on spraying conditions and contact quality, according to Heichal et al. Furthermore, they acknowledged the difficulty of measuring the resistance through thermal contact along the splat–substrate surface as it fluctuates and advised using a constant number instead (Heichal and Chandra 2005).

The part of wetting for ceramic particles being thermally sprayed on various substrate surfaces was explored by Fukumoto et al. They found that increased wettability at the splat–substrate interface encourages disk-shaped splats. They also suggested that good wettability impacts particles'

ability to flatten and stick effectively to the final target surface. It was also noted that thermodynamically unstable oxides increase the chances of wetting on any metal/metal oxide combination. Metal/metal systems also have a lighter transition temperature than ceramic or metal systems (Fukumoto et al. 2007).

Effect of transition temperature on droplet flattening

The most promising parameter at the liquid splat–substrate interface is bonding temperature during splat formation regarding the available less time. According to Fukumoto et al. (2007), the transformation of disk splats to splash splats can happen quickly under pressure and materials transition temperature parameters. The material transition temperature is suggested at a range that amplifies the splat frequency by 50% or more alongside substrate heating. The transition pressure is the pressure (below the material critical pressure) at which metallic particle splat morphologies such as Ni, Ti, Al, Cu, and others are altered. They suggest that preheating substrate over the transition temperature significantly impacts adhesive strength. They also proposed that transition pressure could improve the adhesion properties of some systems.

Mantry et al. (2014) investigated the effects of several spraying parameters. They observed that the impact velocity of sprayed particles, temperature, and impact angle of particles are important determinants in coating performance. The ratio of plasma gas to carrier gas flow rate for feeding feed stock (powder), according to Mihm et al. (2012), is a significant component in determining coat quality. An increase in plasma jet temperature was observed with the increase in plasma gas, while an increase in carrier gas flow rate aids the powder's entry into the plasma jet's center. The plasma jet will bend out of its typical position at a high carrier gas flow rate, resulting in a non-uniform coating thickness distribution and poor deposition efficiency. Schulz et al. (2007) considered the influence of substrate rotation on coating growth during vapor-phase deposition by varying the vapor impact angle on the substrate surface at the same temperature. Increased substrate rotation can cause morphological changes and increased grain growth behavior in columnar grains. Kuanr et al. (2018) discovered that TBC deposition at a substrate temperature of 100 °C provides the highest thermal conductivity compared to substrates at temperatures greater than 100 °C.

The influence of substrate temperature on TBC surface roughness was examined by Jesuraj et al. (2018). It was discovered that as the substrate temperature rises, the surface roughness also increases. Morks et al. (2002) investigated the influence of the pressure of the chamber and found that the morphology of CI material splats changed from star-type to disk-type shape as the chamber pressure varied. Low chamber pressure successfully eliminated the volumes of condensates by decreasing the vapor pressure, which hastened its evaporation and resulted in a smooth substrate surface.

Even though several scholars have presented different suggestions based on their experimental findings, there has yet to be a consensus on the process that creates splashing or disk splats under varied settings. Parameters like surface chemistry, roughness, oxides at the surface, temperatures of substrate and splat, transition temperature/pressure, wettability, cooling rate and rate of solidification, and other characteristics have been studied for this purpose. To increase the essential knowledge of reactive wetting and consequent impact of interfacial reactions on flattening and splat spreading, it is necessary to explore these interfacial reactions' real role and kinetics in various systems.

Role and importance of wetting

Wetting has been believed to be the most significant metric due to its critical technical value in a broad range of manufacturing applications. It has grown in relevance over the previous decade because it is one of the main essential characteristics that define coating quality. Many academics have underlined the importance of wetting and suggested that it is the most significant aspect of the coating process. Wetting is the process of a liquid droplet spreading across a solid surface. Reactive wetting and non-reactive wetting have been recognized in the literature as two primary forms of wetting. The chemical response at the substrate surface is the primary criterion for distinguishing the two. Reactive wetting (Agarwal et al. 2022) is advocated when the substrate conducts any reaction/absorption, whereas inert or non-reactive wetting (Eustathopoulos and Voytovych 2016) is recommended when the substrate does not react. Reactive wetting, it is inferred, changes the contact and induces the development of new intermetallic compounds on it. Various characteristics that affect reactive wetting, like diffusion, absorption, reaction, and solidification, have been proposed. The reactive wetting is usually related to reactive metals on ceramic substrates metal. Because of their reactive nature, these reactive metals trigger severe reactions on substrate surfaces, affecting coating quality (Kumar and Prabhu 2007; Šikalo et al. 2005). According to Kumar et al., liquid parameters, substrate qualities, and system circumstances all play a part in spreading. Certain studies have categorized wetting depending on the driving forces that cause it, such as spontaneous and forced wetting. The term "spontaneous wetting" refers to the spread of a sprayed droplet due to gravity or capillary processes, whereas "forced wetting" refers to

the spread of a sprayed droplet under controlled conditions (Kumar and Prabhu 2007).

Two characteristics have been detailed repeatedly in the literature: wetting degree and rate, which are useful in characterizing the wetting phenomena. The wetting degree is determined by contact angle measurement at the solid–liquid surface interface, influenced by numerous characteristics such as surface and interfacial energy. Many studies have utilized the contact angle measurement approach to explore wetness in various processes, proposing that the contact angle should be less than 90° for complete wetting and zero in optimal conditions. The contact angle is defined as the angle formed by the triple point tangents and substrate surface (Kumar and Prabhu 2007; Liu et al. 2010).

Contact angle calculation is now used to research wetting/dewetting, characterize interfacial processes, coat surfaces, etc. To date, various methodologies for measuring the contact angle have been devised. The well-known methods used by different studies include sessile drop and wetting balancing procedures and optical measurements. Typically, these procedures measure contact angles under controlled and established settings. The types of contact angles available in the literature are included in Table 2 (Karim et al. 2018).

On the other hand, the wetting rate is approached by the spreading droplet speed. The wetting rate is influenced by several additional factors, including the system's temperature condition, capillary forces, viscosity, and chemical reactions at substrate interfaces. The equation (Young–Dupre) (Benkreif et al. 2021) is used to characterize inert environments' wetting process by measuring the contact angle. It increases coating adhesion strength due to improved substrate and splat connection.

$$W_{sl} = \gamma_l(1 + \cos\theta) \tag{4}$$

where W_{sl} represents adhesion work and γ_l is interfacial tension among the solid and liquid phases. As of this equation result, it is suggested that the work of adhesion must be twice the tension at the interface for the perfect wetting case. Wetting balance and sessile drop techniques are widely utilized to examine the angle of contact for chemically inactive systems. The literature has presented the coefficient of spreading "*S*" of classical Young–Dupre equation to manage when the contact angle may come at zero, and Young's equation (Ismail et al. 2021) can become unacceptable.

$$S = \gamma_{sv} - (\gamma_{sl} + \gamma_{lv}) = \gamma_{lv}(\cos\theta - 1) \tag{5}$$

The above-mentioned spreading coefficient must be positive or zero for complete wetting. Contact angle measurement has not been accepted for reactive systems because of the multiple parameters involved in the reactions at interfaces. Many researchers presented various explanations, but none fully explained the occurrence. The hysteresis contact angles can be computed using disjoining/conjoining pressure, according to Arjmandi-Tashet et al. According to the theory, the equilibrium contact angle is closer to a static retreating contact angle than a static advancing contact angle. McDonald et al. found that the change in Gibbs free energy is critical in controlling wetting in any metal/ceramic combination (McDonald et al. 2007b).

The relationship between interfacial composition and wetting was investigated for CuAg alloys with a small percentage of Ti on alumina substrates, a highly interesting combination in alumina component brazing (Kozlova et al. 2010). The sessile drop experiment in Fig. 8 illustrates the influence of Ti on wetting. A CuAg-1.75wt% Ti alloy was treated in situ by dropping a small amount of Ti on the upper surface of AgCu on an alumina substrate (Voytovych et al. 2006).

Replacement of the alumina piece with a Cu–Ni plate, the Ni and Cu from the plate dissolve in the liquid braze, causing considerable change not only in joint microstructure, but alumina/braze interface reactivity also changes, consisting of a one-order-of-magnitude reduction in the interfacial reaction layer thickness (from 2 m to 200 nm). Furthermore, in the CuNi/alumina joint, high oxidation-level *Ti* oxides form at the interfaces rather than wettable Cu_3Ti_3O compound developed at the interfaces in the Al_2O_3-to- Al_2O_3 joint, resulting in an appreciable enhancement in contact

Table 2 Types of contact angles

Contact angles		Definition
Static contact angles	Contact angle (Intrinsic)	The angle at the ideal or perfect solid surface
	Contact angle (Equilibrium/Young's)	Angle observed due to tension forces at the surface
	Contact angle (Wenzel)	Contact angle observed between homogeneous and irregular solid surface
	Contact angle (Cassie)	Contact angle observed at heterogeneous and fine solid surface
Dynamic contact angles	Contact angle (Apparent)	Contact angle observed on a solid surface
	Contact angle (Quasi-equilibrium)	Contact angle at a metastable state system with insignificant variation
	Contact angle (Advancing)	Angle is achieved when the rate volume of the droplet is declining
	Contact angle (receding)	Angle achieved when the rate of volume of droplet increased

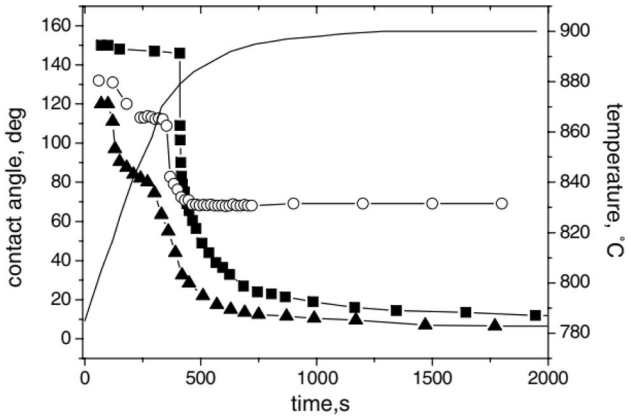

Fig. 8 Variation in contact angle with respect to time for two droplets of CuAgTi having different compositions measured in situ on monocrystalline alumina in helium at 900 °C adapted from Voytovych et al. (2006)

angle and thus resulting in weak mechanical interface and the actual joint (Valette et al. 2005).

Instead of the physicochemical nature of the interfaces, according to Fujji et al., Gibbs's free reaction energy at the surface interface plays a crucial part in any researched system. He demonstrated that the Al/AlN and Al/BN systems support the quiet function of interface physicochemical characteristics. As discussed in the Al/BN system, AlN is regarded as the interfacial product, having zero contact angle. In the matching experiment, the Al/AlN system had a contact angle of 130°, which contradicts the type of the interfacial product layer hypothesis because if it were valid, contact angles would have been identical in both systems (Fujii and Nakae 1996). After decades of research in reactive wetting, it has been deduced that any reactive system consists of the following steps (Kozlova et al. 2011).

- The process of rapid spreading occurs.
- Quasi-equilibrium is attained.
- Interfacial front advance.
- Decrease in the height of the droplet.
- The equilibrium stage of wetting.

When Tanaka et al. investigated the effect of wetting on thermally sprayed Al_2O_3 powder on AISI304 (Au coated via PVD) substrate, they came to the same conclusion. He believes improving wettability can achieve consistent coating quality (Tanaka and Fukumoto 1999). Though much research has been done to clarify the role of wetness, there is still a lot to learn. Much of the literature fulfills either in a controlled, conditioned environment (vacuum, inert) or in other certain parameters like PVD coatings, higher temperatures, and so on; however, in real-world spraying situations, coatings are more complicated and influenced by various parameters. As a result, the intricacy of the real-world process forces researchers to dig deeper into this component, resulting in better coating quality.

According to the literature, substrate roughness, temperature, trace elements, atmospheric conditions, droplet characteristics, and other physical and non-physical factors all play a role in reactive wetting. As a result, taking these aspects into account when evaluating the wetness is crucial (Li 1994). Rough surfaces, it is thought, give more interfacial area and, by raising surface energy, may promote wetting. Wenzel began by presenting the equation which shows the relationship between the equilibrium and apparent angle of contact (Azadi Tabar et al. 2019). Later, Hitchcock established the below expression that meaningfully accounts for the impacts on wetting of roughness.

$$r = 1 + C_1(R/\lambda)^2 \tag{6}$$

$$\alpha = \tan^{-1}(C_2 R/\lambda) \tag{7}$$

where α shows the angle of tilt, r shows Wenzel's roughness, R depicts root mean square roughness surface height, and λ is the average distance between asperities of rough surface (Nosonovsky 2007). Since then, some research has been executed to discover the impact of wetting on roughness. In reactive nature wetting, surface roughness is key in providing supplementary sites for adsorption, diffusion, reaction, and nucleation.

Impact of interfacial products on reactive wetting

According to a large body of the literature on the subject, the existence of interfacial chemicals in any system has a substantial impact on the wetting process. In many cases, substrate melting has hastened the creation of intermetallic compounds, according to the literature. These compounds are said to be the direct outcome of interface reactions triggered by the melting of substrate or substrate surface heterogeneity, such as the existence of an oxide layer. Other parameters, such as the factor of substrate roughness, reactive elements, and temperature of the substrate, have also been identified as regulating aspects for creating these compounds of intermetallic nature. A lot of evidence has been submitted to date about the presence of these newly formed interfacial compounds at interfaces. Still, their legitimacy has been questioned because some have identified a major layer of these compounds, i.e., a few microns. In contrast, others have only reported their role at nanometers or atomic scales (Dezellus and Eustathopoulos 2010; Protsenko et al. 2001). Hence, these compounds' formation and their role in influencing the wettability of liquid droplets on the substrate surface are still under conversation.

Protsenko et al. used the dispensed drop method to study metal–metal systems and rejected the hypothesis of better wetting through the release of reaction energy due to compound formation at the interface. Furthermore, he hypothesized that intermetallic compound production for oxidized substrates aids wetting by removing the oxide coating from the substrate and giving the spreading liquid a new clean surface of the final product. He went on to say that when powerful reactions happen at the interface, wetness becomes less susceptible to external influences (Protsenko et al. 2001). According to Yin et al., compound production of intermetallic nature at the triple line can stymie triple line progression by halting the spreading of bulk liquid in a controlled (formic acid chamber environment) dissolutive wetting system. He argued that in such systems, the creation of intermetallic compounds at the triple line regulates wetting because these compounds reduce the velocity of the triple line, which slows the spreading on the substrate surface. He further asserts that creating intermetallic compounds at the solid–liquid interface impedes substrate disintegration. As a result, interfacial interactions are critical in wetting and spreading droplets on substrate surfaces (Yin et al. 2008).

Brossard et al. confirmed the existence of intermetallic compound production at the interface after thermal spraying NiCr alloy powder on an aluminum substrate. Their findings revealed that flow at interfaces containing elements (Ni, Al) from both the splat and the substrate material resulted in metastable phases (Al rich and Ni rich) and different oxides. The same findings were claimed by Chraska et al. for thermal spraying of YSZ (7wt%) on material stainless steel 316 substrates. A thermally developed oxide layer with a thickness of 20-30nm at warmed SS-316 substrate interface was revealed by TEM examinations of interfaces, which assisted wetting during the process (Chraska and King 2002).

Bian et al. used the sessile drop method to observe the reactive wetting behavior of zirconia with SnAgCu-x percent Ti alloy (Bian et al. 2019). According to kinetic estimates, interfacial reaction governed the SAC-Ti droplets, spreading on the zirconia surface. The inclusion of Ti significantly impacts the distribution and shape of reaction products in droplets. Due to droplets' limited spreading and fluidity, a large amount of Ti-Sn intermetallic compounds was created in droplets as the Ti concentration increased from 1 to 4%. As a result, the contour of droplets changed from hemispherical to comparable trapezoidal. The wettability of SAC-Ti/zirconia was considerably improved due to the interfacial reaction between active elements Ti and zirconia and the subsequent creation of the Ti–O layer. The literature shows that much effort has been made on static systems with controlled circumstances to examine contact phenomena. These compounds' intermetallic nature enhances the reactive wetting property by eliminating existing oxides at the surface of a substrate and creating a newly polished surface for recently produced materials (Dezellus and Eustathopoulos 2010). Protsenko et al. investigated the function of intermetallic compounds on reactive wetting conditions under controlled settings. They concluded that these discussed compounds offer adequate conditions for process, particularly in metal-to-metal systems. Their findings included considerable effects of substrate conditions, while it was reported that roughness could only promote wetting until it reaches a threshold point. (Protsenko et al. 2001).

According to Liang et al., metal/ceramic systems are generally regulated by chemical reactions at the interface. In contrast, dissolutive wetting systems are controlled by solute diffusion that normally begins at the solid–liquid adjacent line and moves near the contact line. This rich solute-containing flow flows toward the liquid–vapor boundary, but no compound formation occurs in the early stages of spreading (Yin et al. 2006). Andrieux et al. identified compound formation at the interface at solid and liquid interfaces when engaged on liquid Ag–Cu eutectic alloys and solid titanium in variable vacuum conditions. They identified product layers after a metallographic examination that confirmed the presence of layers of product in favorable conditions. He also claimed the occurrence of various layers of product, which he said improved wetting and offered clear evidence of typical advancement in the final material (Andrieux et al. 2009).

Zhang et al. fabricated the Fe-based amorphous coatings on the surface of a WE43 substrate by high-velocity oxy-fuel thermal spraying at optimized thermal inputs. They found that at high-velocity oxy-fuel spray particles' high impact velocity and cooling rate, coating 2 was well formed at high thermal inputs and still maintained 92.5% high amorphous fraction. A dense interlayer was formed between the coating and the substrate using Ni60 particles firmly bound with WE43 and Fe-based amorphous particles. It is confirmed that there was a fracture within the coating, and coating 2's bonding strength reached 56.11 MPa due to the spray particles' metallurgical bonding and mechanical interlocking effect (Zhang et al. 2021).

Low adhesion strength is caused by cracks that form at unfused particle boundaries and spread over the coating/substrate contact. Improving bonding relies mostly on adhesion interlayers that improve particle wettability to overcome this. Coatings with a solitary NiCrAl interlayer and a layered coating/interlayer design, for example, were applied to AISI 1045 mild steel surfaces, providing a significant bonding strength of roughly 40 MPa. Surprisingly, fractures were confined around the coating interface, with crystalline interlayer phases acting as efficient barriers to crack propagation. This work underscores the significance of strategic interlayer use and sheds light on fracture mechanisms in adhesion processes (Zhang et al. 2014; Peng et al. 2013).

Importance of additives or reactive elements in wetting

Including specific components has been noted to alter wetting in the literature. A plethora of elements has been included as additives or reactive elements to make alloys for improved mechanical or wetting qualities in soldering alongside brazing. These additives are thought to provide a reaction product that aids in wetting alloy (soldering/brazing) on the substrate surface (Kumar and Prabhu 2007). Nicholas et al. (1980) used the sessile drop method to study the wetting of alumina by copper–titanium alloys and found that due to the titanium addition, the wetting behavior changed from non-wetting to wetting and the contact angle fell to 72° from 138°. In a sessile drop test, Sandra et al. found similar results, where copper–chromium alloys demonstrated better wetting on a graphite substrate. A substantial reaction layer (10 m) and a lowered contact angle of 41° were noted. They hypothesized that copper, rather than graphite, effectively wets the reaction product layer and improves wetting significantly (Devincent and Michal 1993).

The interfaces created between liquid tin and vanadium alloys on alumina were described by Win et al., who claimed that some nanoscale mixed oxide (AlV_2O_4) layer was deposited at the interface. Researchers also claimed that segregation of vanadium took place on the interface, forming a layer at the interface containing solely rich vanadium oxides. They showed a schematic in Fig. 9 of interface creation in the alumina system and liquid Sn–V alloy (Winn et al. 2004).

Naidich et al. established that the freshly generated compound layer is not solely responsible for the level of system's wetting, including Ti and Cr, considered reactive elements. He also claims that adding reactive elements promotes oxide formation in metal–ceramic systems by wetting them until they are in a bulk liquid state and have high oxygen affinity. He also stated that if this newly generated product layer plays a part in wetting effectively, it should comprise only a few atomic layers (nanometers) (Naidich 2005).

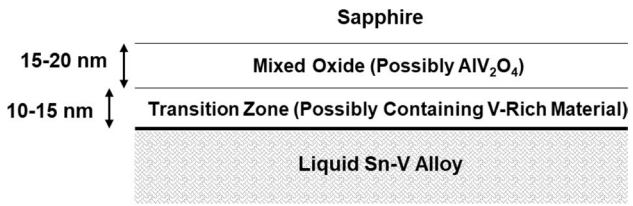

Fig. 9 Schematic of Sn-V alloy's internal structure of interface formation on alumina adapted with permission from Winn et al. (2004)

Future recommendations

As previously stated, relevant data had been published exclusively for the static systems, where interfacial chemicals had been identified in millimeter-sized liquid droplets under situations. These findings have been proposed for real-world applications like spraying, where operating conditions are more vibrant. Because the reaction kinetics at the contact stays the same, sometimes this analogy is ambiguous because powders being thermally sprayed are not millimeter-sized, nor does the reaction take as long to complete as it does under stationary conditions. Even though plenty of researchers have investigated this issue of interfacial formation of the compound and its implications on the wettability of the following processes, no comprehensive approach to dealing with all couples of material systems has been created so far. Many problems remain unresolved when it comes to the processes being dynamic (such as spraying), rather than stationary ones (Chellaganesh et al. 2021).

Additionally, it might be argued that finding a monolithic coating in any of the applications mentioned above that can "overcome" the design constraints is a significant difficulty (Gildersleeve and Vaßen 2023). More advanced and creative coating solutions will become standard operating procedures as industry awareness of and adoption of thermal spray technology grows. For instance, cold spray rivals earlier thermal spray techniques in creating coatings with excellent corrosion and wear resistance (Singh et al. 2023). In order to maximize economic and productivity gains, the steel sector should also investigate thermal spray's on-site repair capabilities.

In order to cut pollution and waste, artificial intelligence (AI) and machine learning have become more popular in other industries. Thermal spray can contribute to this development (Sarc et al. 2019). Additionally, robots are primarily utilized in thermal spray procedures to direct the movement of the spray torch to produce complex shapes and guarantee a secure working environment. Robotic automation integration results in high-quality and reasonably priced coatings while giving the manufacturing process flexibility and reproducibility. Therefore, integrated automation and thermal spray procedures make faster on-site repairs of damaged components possible. Decreasing production downtime increases the productivity of the steel manufacturing industry (Gadow and Floristán 2015; Bocklisch et al. 2022). To determine the optimum approach for an efficient coating, machine learning could let robot pathways be smoothly learned and modified (Ikeuchi et al. 2019; Viswanathan et al. 2021). As a result, the need to generate considerable data for dynamic wetting processes while including significant influencing factors

necessitates more research in the above area, which will undoubtedly contribute to technological advancement and future research.

Declarations

Conflict of interest On behalf of all authors, the corresponding author states that there is no conflict of interest. Moreover, the authors have no relevant financial or non-financial interests to disclose. The authors have no competing interests to declare relevant to this article's content.

References

Agarwal H, Breining WM, Sánchez-Velázquez G, Lynn DM (2022) Reactive multilayers and coatings fabricated by spray assembly: influence of polymer structure and process parameters on multiscale structure and interfacial properties. Chem Mater 34:1245–1258

Ahmed A, Mhaede M, Wollmann M, Wagner L (2015) Characteristics of sintered HA coating deposited by chemical method on AISI 316L substrate. Mater Des 76:9–17

Amado J, Montero J, Tobar M, Yáñez A (2012) Ni-based metal matrix composite functionally graded coatings. Phys Procedia 39:362–367

Andrieux J, Dezellus O, Bosselet F, Viala J (2009) Low-temperature interface reaction between titanium and the eutectic silver-copper brazing alloy. J Phase Equilib Diffus 30:40–45

Ann Gan J, Berndt CC (2015) 23 - Thermal spray forming of titanium and its alloys. In: Qian M, Froes FH (eds) Titanium powder metallurgy. Butterworth-Heinemann, Boston, pp 425–446

Armster SQ, Delplanque JP, Rein M, Lavernia EJ (2002) Thermo–fluid mechanisms controlling droplet based materials processes. Int Mater Rev 47:265–301

Arrabal R, Pardo A, Merino M, Mohedano M, Casajús P, Merino S (2010) Al/SiC thermal spray coatings for corrosion protection of Mg–Al alloys in humid and saline environments. Surf Coat Technol 204:2767–2774

Azadi Tabar M, Barzegar F, Ghazanfari MH, Mohammadi M (2019) On the applicability range of Cassie-Baxter and Wenzel equation: a numerical study. J Braz Soc Mech Sci Eng 41:1–12

Aziz SD, Chandra S (2000) Impact, recoil and splashing of molten metal droplets. Int J Heat Mass Transf 43:2841–2857

Baghal SL, Sohi MH, Amadeh A (2012) A functionally gradient nano-Ni–Co/SiC composite coating on aluminum and its tribological properties. Surf Coat Technol 206:4032–4039

Banthia S, Amid M, Sengupta S, Das S, Das K (2020) Reciprocating sliding wear of Cu, Cu–SiC functionally graded coating on electrical contact. J Mater Eng Perform 29:3930–3940

Benkreif R, Brahmia FZ, Csiha C (2021) Influence of moisture content on the contact angle and surface tension measured on birch wood surfaces. Eur J Wood Wood Prod 79:907–913

Bertrand G, Bertrand P, Roy P, Rio C, Mevrel R (2008) Low conductivity plasma sprayed thermal barrier coating using hollow psz spheres: correlation between thermophysical properties and microstructure. Surf Coat Technol 202:1994–2001

Bhusal S, Zhang C, Bustillos J, Nautiyal P, Boesl B, Agarwal A (2019) A computational approach for predicting microstructure and mechanical properties of plasma sprayed ceramic coatings from powder to bulk. Surf Coat Technol 374:1–11

Bian H, Zhou Y, Song X, Hu S, Shi B, Kang J et al (2019) Reactive wetting and interfacial characterization of ZrO2 by SnAgCu–Ti alloy. Ceram Int 45:6730–6737

Blanchi L, Grimaud A, Blein F, Lucchèse P, Fauchais P (1995) Comparison of plasma-sprayed alumina coatings by RF and DC plasma spraying. J Therm Spray Technol 4:59–66

Bocklisch F, Paczkowski G, Zimmermann S, Lampke T (2022) Integrating human cognition in cyber-physical systems: a multidimensional fuzzy pattern model with application to thermal spraying. J Manuf Syst 63:162–176

Bolelli G, Lusvarghi L, Giovanardi R (2008) A comparison between the corrosion resistances of some HVOF-sprayed metal alloy coatings. Surf Coat Technol 202:4793–4809

Brossard S, Munroe P, Tran A, Hyland M (2010a) Study of the splat-substrate interface for a NiCr coating plasma sprayed onto polished aluminum and stainless steel substrates. J Therm Spray Technol 19:24–30

Brossard S, Munroe P, Tran A, Hyland M (2010b) Study of the microstructure of NiCr splats plasma sprayed on to stainless steel substrates by TEM. Surf Coat Technol 204:1608–1615

Brossard S, Munroe PR, Tran ATT, Hyland MM (2010c) Effects of substrate roughness on splat formation for Ni–Cr particles plasma sprayed onto aluminum substrates. J Therm Spray Technol 19:1131–1141

Browning J (1992) Hypervelocity impact fusion—a technical note. J Therm Spray Technol 1:289–292

Campo M, Carboneras M, López M, Torres B, Rodrigo P, Otero E et al (2009) Corrosion resistance of thermally sprayed Al and Al/SiC coatings on Mg. Surf Coat Technol 203:3224–3230

Cedelle J, Vardelle M, Pateyron B, Fauchais P (2005) Investigation of plasma sprayed coatings formation by visualization of droplet impact and splashing on a smooth substrate. IEEE Trans Plasma Sci 33:414–415

Cedelle J, Vardelle M, Fauchais P (2006) Influence of stainless steel substrate preheating on surface topography and on millimeter-and micrometer-sized splat formation. Surf Coat Technol 201:1373–1382

Chandra S, Fauchais P (2009) Formation of solid splats during thermal spray deposition. J Therm Spray Technol 18:148–180

Chatha SS, Sidhu HS, Sidhu BS (2013) High-temperature behavior of a NiCr-coated T91 boiler steel in the platen superheater of coal-fired boiler. J Therm Spray Technol 22:838–847

Chellaganesh D, Khan MA, Jappes JW (2021) Thermal barrier coatings for high temperature applications—a short review. Mater Today Proc 45:1529–1534

Chraska T, King AH (2002) Effect of different substrate conditions upon interface with plasma sprayed zirconia—a TEM study. Surf Coat Technol 157:238–246

Ctibor P, Lechnerová R, Beneš V (2006) Quantitative analysis of pores of two types in a plasma-sprayed coating. Mater Charact 56:297–304

Cui Y, Shen J, Geng K, Hu S (2021) Fabrication of FeCoCrNiMnAl0.5-FeCoCrNiMnAl gradient HEA coating by laser cladding technique. Surf Coat Technol 412:127077

Davis J (2001) Surface engineering for corrosion and wear resistance, ASM international and IOM communications. Maney Publishing, Materials Park (OH)

Davis JR (2004) Handbook of thermal spray technology. ASM international

de la Roche J, Alvarado-Orozco JM, Gómez PA, Cano IG, Dosta S, Toro A (2022) Hot corrosion behavior of dense CYSZ/YSZ bilayer coatings deposited by atmospheric plasma spray in Na2SO4+ V2O5 molten salts. Surf Coat Technol 432:128066

Deng C, Kim H, Ki H (2019) Fabrication of functionally-graded yttria-stabilized zirconia coatings by 355 nm picosecond dual-beam pulsed laser deposition. Compos B Eng 160:498–504

Deng Z, Liu D, Xiong Y, Zhu X, Mi H, Liu J et al (2021) Laser cladding preparation of HA-Ag gradient bioactive ceramic coating: a feasibility study. Surf Coat Technol 427:127848

Devincent SM, Michal GM (1993) Reaction layer formation at the graphite/copper-chromium alloy interface. Metall Trans A 24:53–60

Dezellus O, Eustathopoulos N (2010) Fundamental issues of reactive wetting by liquid metals. J Mater Sci 45:4256–4264

Dhiman R, Chandra S (2005) Freezing-induced splashing during impact of molten metal droplets with high Weber numbers. Int J Heat Mass Transf 48:5625–5638

Dhiman R, McDonald AG, Chandra S (2007) Predicting splat morphology in a thermal spray process. Surf Coat Technol 201:7789–7801

Donaldson L (2021) New optical coating increases the lifetime of photovoltaic cells. Elsevier

Dongmian Z, Xiaowei X (2020) Ceramics coated metallic materials: methods, properties and applications. In: Mohsen M (ed) Advanced ceramic materials. Rijeka, IntechOpen

Eustathopoulos N, Voytovych R (2016) The role of reactivity in wetting by liquid metals: a review. J Mater Sci 51:425–437

Fanicchia F, Maeder X, Ast J, Taylor A, Guo Y, Polyakov M et al (2018) Residual stress and adhesion of thermal spray coatings: microscopic view by solidification and crystallisation analysis in the epitaxial CoNiCrAlY single splat. Mater Des 153:36–46

Fantozzi D, Matikainen V, Uusitalo M, Koivuluoto H, Vuoristo P (2017) Chlorine-induced high temperature corrosion of Inconel 625 sprayed coatings deposited with different thermal spray techniques. Surf Coat Technol 318:233–243

Fathi R, Ma A, Saleh B, Xu Q, Jiang J (2020) Investigation on mechanical properties and wear performance of functionally graded AZ91-SiCp composites via centrifugal casting. Mater Today Commun 24:101169

Fauchais P (2004) Understanding plasma spraying. J Phys D Appl Phys 37:R86

Fauchais P, Vardelle A, Vardelle M, Fukumoto M (2004) Knowledge concerning splat formation: an invited review. J Therm Spray Technol 13:337–360

Fauchais P, Montavon G, Bertrand G (2010) From powders to thermally sprayed coatings. J Therm Spray Technol 19:56–80

Fauchais PL, Heberlein JV, Boulos MI (2014) Industrial applications of thermal spraying technology. Thermal spray fundamentals. Springer, pp 1401–1566

Fujii H, Nakae H (1996) Equilibrium contact angle in the magnesium oxide/aluminium system. Acta Mater 44:3567–3573

Fujimoto H, Shiotani Y, Tong AY, Hama T, Takuda H (2007) Three-dimensional numerical analysis of the deformation behavior of droplets impinging onto a solid substrate. Int J Multiph Flow 33:317–332

Fukumoto M, Huang Y (1999) Flattening mechanism in thermal sprayed nickel particle impinging on flat substrate surface. J Therm Spray Technol 8:427–432

Fukumoto M, Ohgitani I, Yasui T (2004) Effect of substrate surface change on flattening behaviour of thermal sprayed particles. Mater Trans 45:1869–1873

Fukumoto M, Yamaguchi T, Yamada M, Yasui T (2007) Splash splat to disk splat transition behavior in plasma-sprayed metallic materials. J Therm Spray Technol 16:905–912

Gadow R, Floristán M (2015) Manufacturing engineering in thermal spraying by advanced robot systems and process kinematics. Future development of thermal spray coatings. Elsevier, pp 259–280

Galedari SA, Mahdavi A, Azarmi F, Huang Y, McDonald A (2019) A comprehensive review of corrosion resistance of thermally-sprayed and thermally-diffused protective coatings on steel structures. J Therm Spray Technol 28:645–677

Garcia E, Miranzo P, Soltani R, Coyle TW (2008) Microstructure and thermal behavior of thermal barrier coatings. J Therm Spray Technol 17:478–485

Ghadami F, Aghdam ASR, Ghadami S (2020) Preparation, characterization and oxidation behavior of CeO2-gradient NiCrAlY coatings applied by HVOF thermal spraying process. Ceram Int 46:20500–20509

Ghanavati R, Naffakh-Moosavy H, Moradi M (2021) Additive manufacturing of thin-walled SS316L-IN718 functionally graded materials by direct laser metal deposition. J Market Res 15:2673–2685

Gildersleeve EJ, Vaßen R (2023) Thermally sprayed functional coatings and multilayers: a selection of historical applications and potential pathways for future innovation. J Therm Spray Technol 32:778–817

Goutier S, Vardelle M, Fauchais P (2013) Comparison between metallic and ceramic splats: influence of viscosity and kinetic energy on the particle flattening. Surf Coat Technol 235:657–668

Grammes T, Emmerich T, Aktaa J (2021) W/EUROFER functionally graded coatings for plasma facing components: technology transfer to industry and upscaling. Fusion Eng Des 173:112940

Grimm M, Drehmann R, Lampke T, Conze S, Berger L-M (2021) Microstructure of atmospheric plasma sprayed (Al, Cr) 2O3–TiO2 coatings from blends. In *ITSC2021*, pp 758–764

Harun W, Asri R, Alias J, Zulkifli F, Kadirgama K, Ghani S et al (2018) A comprehensive review of hydroxyapatite-based coatings adhesion on metallic biomaterials. Ceram Int 44:1250–1268

Heichal Y, Chandra S (2005) Predicting thermal contact resistance between molten metal droplets and a solid surface. J Heat Transf 127:1269–1275

Herman H, Sampath S, McCune R (2000) Thermal spray: current status and future trends. MRS Bull 25:17–25

Hu X, Li F, Shi D, Xie Y, Li Z, Yin F (2020) A design of self-generated Ti–Al–Si gradient coatings on Ti–6Al–4V alloy based on silicon concentration gradient. J Alloy Compd 830:154670

Hussain T, Dudziak T, Simms N, Nicholls J (2013) Fireside corrosion behavior of HVOF and plasma-sprayed coatings in advanced coal/biomass co-fired power plants. J Therm Spray Technol 22:797–807

Ikeuchi D, Vargas-Uscategui A, Wu X, King PC (2019) Neural network modelling of track profile in cold spray additive manufacturing. Materials 12:2827

Ismail MF, Islam MA, Khorshidi B, Sadrzadeh M (2021) Prediction of surface charge properties on the basis of contact angle titration models. Mater Chem Phys 258:123933

Jesuraj SA, Kuppusami P, Dharini T, Panda P, Devapal D (2018) Effect of substrate temperature on microstructure and nanomechanical properties of Gd2Zr2O7 coatings prepared by EB-PVD technique. Ceram Int 44:18164–18172

Jia M, Chen F, Wu Y, Xu L, Shen Q, Jiang N et al (2022) Microstructure and shear fracture behavior of Mo/AlN/Mo symmetrical compositionally graded materials. Mater Sci Eng, A 834:142591

Jiang X, Wan Y, Herman H, Sampath S (2001) Role of condensates and adsorbates on substrate surface on fragmentation of impinging molten droplets during thermal spray. Thin Solid Films 385:132–141

Jones H (1971) Cooling, freezing and substrate impact of droplets formed by rotary atomization. J Phys D Appl Phys 4:1657–1660

Kadam NR, Karthikeyan G, Kulkarni DM (2019) Microstructure and mechanical properties of atmospheric plasma sprayed 8YSZ thermal barrier coatings. Advances in micro and nano manufacturing and surface engineering. singapore, pp 437–446

Kadam NR, Karthikeyan G, Kulkarni DM (2020) Effect of substrate rotation on the microstructure of 8YSZ thermal barrier coatings by EB-PVD. Mater Today Proc 28:678–683

Kadam NR, Karthikeyan G, Kulkarni DM (2022a) The effect of spray angle on the microstructural and mechanical properties of plasma sprayed8YSZ thermal barrier coatings. J Micromanuf 52(2):181–192

Kadam NR, Karthikeyan G, Jagtap PM, Kulkarni DM (2022b) An atmospheric plasma spray and electron beam-physical vapour deposition for thermal barrier coatings: a review. Aust J Mech Eng. https://doi.org/10.1080/14484846.2022.2030088

Karim AM, Rothstein JP, Kavehpour HP (2018) Experimental study of dynamic contact angles on rough hydrophobic surfaces. J Colloid Interface Sci 513:658–665

Kiilakoski J, Puranen J, Heinonen E, Koivuluoto H, Vuoristo P (2019) Characterization of powder-precursor HVOF-Sprayed Al2O3-YSZ/ZrO2 coatings. J Therm Spray Technol 28:98–107

Klinkov S, Kosarev V (2006) Measurements of cold spray deposition efficiency. J Therm Spray Technol 15:364–371

Korobov Y, Nevezhin S, Filippov M, Makarov A, Malygina I, Fantozzi D et al. (2016) Study of high velocity arc sprayed heat resistant coatings from FeCrAlBY cored wire. In Proceedings of the international thermal spray conference, pp 852–856

Kozlova O, Braccini M, Voytovych R, Eustathopoulos N, Martinetti P, Devismes M-F (2010) Brazing copper to alumina using reactive CuAgTi alloys. Acta Mater 58:1252–1260

Kozlova O, Voytovych R, Eustathopoulos N (2011) Initial stages of wetting of alumina by reactive CuAgTi alloys. Scr Mater 65:13–16

Kuanr SK, Vinothkumar G, Babu KS (2018) Substrate temperature dependent structural orientation of EBPVD deposited NiO films and its influence on optical, electrical property. Mater Sci Semicond Process 75:26–30

Kumar G, Prabhu KN (2007) Review of non-reactive and reactive wetting of liquids on surfaces. Adv Coll Interface Sci 133:61–89

Kyhl L, Balog R, Cassidy A, Jørgensen J, Grubisic-Čabo A, Trotochaud L et al (2018) Enhancing graphene protective coatings by hydrogen-induced chemical bond formation. ACS Appl Nano Mater 1:4509–4515

Łatka L, Pawłowski L, Winnicki M, Sokołowski P, Małachowska A, Kozerski S (2020) Review of functionally graded thermal sprayed coatings. Appl Sci 10:5153

Li J-G (1994) Wetting of ceramic materials by liquid silicon, aluminium and metallic melts containing titanium and other reactive elements: a review. Ceram Int 20:391–412

Li C-J, Li J-L (2004a) Evaporated-gas-induced splashing model for splat formation during plasma spraying. Surf Coat Technol 184:13–23

Li C-J, Li J-L (2004b) Transient contact pressure during flattening of thermal spray droplet and its effect on splat formation. J Therm Spray Technol 13:229–238

Li C-J, Liao H-L, Gougeon P, Montavon G, Coddet C (2005) Experimental determination of the relationship between flattening degree and Reynolds number for spray molten droplets. Surf Coat Technol 191:375–383

Li C-J, Yang G-J, Li C-X (2013) Development of particle interface bonding in thermal spray coatings: a review. J Therm Spray Technol 22:192–206

Li C-J, Luo X-T, Yao S-W, Li G-R, Li C-X, Yang G-J (2022) The bonding formation during thermal spraying of ceramic coatings: a review. J Therm Spray Technol 31:780–817

Liang P, Zeng J, Yang X, Zhang H, Dong S, Jiang J et al (2019) Duplex and functionally graded Al@ NiCr/8YSZ thermal barrier coatings on aluminum substrates. J Alloy Compd 790:928–940

Lima RS, Marple BR (2007) Thermal spray coatings engineered from nanostructured ceramic agglomerated powders for structural, thermal barrier and biomedical applications: a review. J Therm Spray Technol 16:40–63

Liu G, Muolo M, Valenza F, Passerone A (2010) Survey on wetting of SiC by molten metals. Ceram Int 36:1177–1188

López A, Proy M, Utrilla V, Otero E, Rams J (2014) High-temperature corrosion behavior of Ni–50Cr coating deposited by high velocity oxygen–fuel technique on low alloy ferritic steel. Mater Des 59:94–102

Madejski J (1976) Solidification of droplets on a cold surface. Int J Heat Mass Transf 19:1009–1013

Mantry S, Sahoo R, Jha BB, Mishra BK, Chakraborty M (2014) Tribo-performance of plasma-sprayed nanostructured yttria-stabilized zirconia coatings using Taguchi's experimental design. Proc Inst Mech Eng Part J J Eng Tribol 228:872–880

McDonald A, Moreau C, Chandra S (2007a) Thermal contact resistance between plasma-sprayed particles and flat surfaces. Int J Heat Mass Transf 50:1737–1749

McDonald A, Moreau C, Chandra S (2007b) Effect of substrate oxidation on spreading of plasma-sprayed nickel on stainless steel. Surf Coat Technol 202:23–33

McPherson R, Shafer B (1982) Interlamellar contact within plasma-sprayed coatings. Thin Solid Films 97:201–204

Meißner TM, Montero X, Fähsing D, Galetz MC (2020) Cr diffusion coatings on a ferritic-martensitic steel for corrosion protection in KCl-rich biomass co-firing environments. Corros Sci 164:108343

Mihm S, Duda T, Gruner H, Thomas G, Dzur B (2012) Method and process development of advanced atmospheric plasma spraying for thermal barrier coatings. J Therm Spray Technol 21:400–408

Milanti A, Matikainen V, Koivuluoto H, Bolelli G, Lusvarghi L, Vuoristo P (2015) Effect of spraying parameters on the microstructural and corrosion properties of HVAF-sprayed Fe–Cr–Ni–B–C coatings. Surf Coat Technol 277:81–90

Miller RA (1987) Current status of thermal barrier coatings—an overview. Surf Coat Technol 30:1–11

Moreau C, Gougeon P, Lamontagne M (1995) Influence of substrate preparation on the flattening and cooling of plasma-sprayed particles. J Therm Spray Technol 4:25–33

Morks M, Tsunekawa Y, Okumiva M, Shoeib M (2002) Splat morphology and microstructure of plasma sprayed cast iron with different preheat substrate temperatures. J Therm Spray Technol 11:226–232

Moskal G, Migas D, Osadnik M, Wrona A (2019) Characterization of the gradient (Mo, Re) Si2/Mo-Re coatings deposited in the hybrid process. J Therm Spray Technol 28:1532–1553

Mundo C, Sommerfeld M, Tropea C (1995) Droplet-wall collisions: experimental studies of the deformation and breakup process. Int J Multiph Flow 21:151–173

Murray JW, Leva A, Joshi S, Hussain T (2018) Microstructure and wear behaviour of powder and suspension hybrid Al2O3–YSZ coatings. Ceram Int 44:8498–8504

Myoung S-W, Kim J-H, Lee W-R, Jung Y-G, Lee K-S, Paik U (2010) Microstructure design and mechanical properties of thermal barrier coatings with layered top and bond coats. Surf Coat Technol 205:1229–1235

Naidich Y (2005) About liquid metal/ceramic interface interaction mechanism and mode of a new intermediate compound formation. Curr Opin Solid State Mater Sci 9:161–166

Nicholas M, Valentine T, Waite M (1980) The wetting of alumina by copper alloyed with titanium and other elements. J Mater Sci 15:2197–2206

Nosonovsky M (2007) On the range of applicability of the Wenzel and Cassie equations. Langmuir 23:9919–9920

Odhiambo JG, Li W, Zhao Y, Li C (2019) Porosity and its significance in plasma-sprayed coatings. Coatings 9:460

Oksa M, Metsäjoki J, Kärki J (2015) Thermal spray coatings for high-temperature corrosion protection in biomass co-fired boilers. J Therm Spray Technol 24:194–205

Pandey SM, Murtaza Q, Walia R (2017) Study of dry wear behavior and morphological characteristic of 60% Mo-20% NiCr-10% CrC-10% Mo+ Fe based alloy coating by atmospheric plasma spray technique. Adv Mater Process Technol 3:393–406

Pandey SM, Murtaza Q, Walia R (2018) Effect of NiCr on dry sliding wear of high carbon iron-molybdenum composite plasma spray coating. Int J Precis Technol 8:1–23

Parmar H, Tucci F, Carlone P, Sudarshan T (2022) Metallisation of polymers and polymer matrix composites by cold spray: state of the art and research perspectives. Int Mater Rev 67:385–409

Peng Y, Zhang C, Zhou H, Liu L (2013) On the bonding strength in thermally sprayed Fe-based amorphous coatings. Surf Coat Technol 218:17–22

Petrova V, Schmauder S (2020) A theoretical model for the study of thermal fracture of functionally graded thermal barrier coatings with a system of edge and internal cracks. Theor Appl Fract Mech 108:102605

Protsenko P, Terlain A, Traskine V, Eustathopoulos N (2001) The role of intermetallics in wetting in metallic systems. Scr Mater 45:1439–1445

Rana N, Mahapatra MM, Jayaganthan R, Prakash S (2015) High-temperature oxidation and hot corrosion studies on NiCrAlY coatings deposited by flame-spray technique. J Therm Spray Technol 24:769–777

Rao H, Jayasekara I, Dutta B, Maurice D (2020) Segregation phenomena during deposition of functionally graded zirconia-based ceramics with Stellite 21 on a steel substrate. Surf Coat Technol 383:125270

Rath PC, Besra L, Singh BP, Bhattacharjee S (2012) Titania/hydroxyapatite bi-layer coating on Ti metal by electrophoretic deposition: characterization and corrosion studies. Ceram Int 38:3209–3216

Rezakhani D (2007) Corrosion behaviours of several thermal spray coatings used on boiler tubes at elevated temperatures. Anti-Corros Methods Mater 54:237–243. https://doi.org/10.1108/00035590710762384

Rousseau F, Guyon C, Morvan D, Bacos MP, Lavigne O, Rio C et al (2021) Low power plasma spray assisted thermal barrier coating repair without the plugging of cooling holes. Surf Coat Technol 412:127050

Sadeghi E, Markocsan N, Joshi S (2019) Advances in corrosion-resistant thermal spray coatings for renewable energy power plants. Part I: effect of composition and microstructure. J Therm Spray Technol 28:1749–1788

Sadeghimeresht E (2018) Ni-based coatings for high temperature corrosion protection. University West

Sadeghimeresht E, Markocsan N, Nylén P (2016) A comparative study on Ni-based coatings prepared by HVAF, HVOF, and APS methods for corrosion protection applications. J Therm Spray Technol 25:1604–1616

Saleh B, Ahmed M (2021) Wear characteristics of functionally graded tubes reinforced with silicon carbide and alumina: a comparative study. Trans Nanjing Univ Aeronaut Astronaut 38:76–83

Saleh B, Jiang J, Fathi R, Al-hababi T, Xu Q, Wang L et al (2020) 30 Years of functionally graded materials: an overview of manufacturing methods, applications and future challenges. Compos B Eng 201:108376

Sarc R, Curtis A, Kandlbauer L, Khodier K, Lorber KE, Pomberger R (2019) Digitalisation and intelligent robotics in value chain of circular economy oriented waste management—a review. Waste Manag 95:476–492

Schulz U, Rätzer-Scheibe H-J, Saruhan B, Renteria AF (2007) Thermal conductivity issues of EB-PVD thermal barrier coatings. Mater Werkst 38:659–666

Shi M, Xue Z, Zhang Z, Ji X, Byon E, Zhang S (2020) Effect of spraying powder characteristics on mechanical and thermal shock properties of plasma-sprayed YSZ thermal barrier coating. Surf Coat Technol 395:125913

Shin K, Acri T, Geary S, Salem AK (2017) Biomimetic mineralization of biomaterials using simulated body fluids for bone tissue engineering and regenerative medicine. Tissue Eng Part A 23:1169–1180

Šikalo Š, Tropea C, Ganić E (2005) Dynamic wetting angle of a spreading droplet. Exp Thermal Fluid Sci 29:795–802

Singh H, Puri D, Prakash S (2005) High temperature oxidation behaviour of plasma sprayed NiCrAlY coatings on Ni-based superalloys in air. Trans Indian Inst Met 59:215

Singh A, Sharma V, Mittal S, Pandey G, Mudgal D, Gupta P (2018) An overview of problems and solutions for components subjected to fireside of boilers. Int J Ind Chem 9:1–15

Singh S, Berndt CC, Singh Raman RK, Singh H, Ang ASM (2023) Applications and developments of thermal spray coatings for the iron and steel industry. Materials 16:516

Song B, Pala Z, Voisey K, Hussain T (2017) Gas and liquid-fuelled HVOF spraying of Ni50Cr coating: microstructure and high temperature oxidation. Surf Coat Technol 318:224–232

Sopronyi M, Nita C, Le Meins J-M, Vidal L, Jipa F, Axente E et al (2021) Laser-assisted synthesis of carbon coatings with cobalt oxide nanoparticles embedded in gradient of composition and sizes. Surf Coat Technol 419:127301

Stathopoulos V, Sadykov V, Pavlova S, Bespalko Y, Fedorova Y, Bobrova L et al (2016) Design of functionally graded multilayer thermal barrier coatings for gas turbine application. Surf Coat Technol 295:20–28

Sun J, Fu Q-G, Li T, Zhang G-P, Yuan R-M (2019) Oxidation behavior of thermally sprayed Mo–Si based composite: effect of metastable phase, porosity and residual stress. J Alloy Compd 776:712–721

Taleghani P, Valefi Z, Ehsani N (2021) Evaluation of oxidation and thermal insulation capability of nanostructured La2 (Zr0· 7Ce0. 3) 2O7/YSZ functionally graded coatings. Ceram Int 47:8915–8929

Talib R, Saad S, Toff M, Hashim H (2003) Thermal spray coating technology: a review. Solid State Sci Technol 11:109–117

Tanaka Y, Fukumoto M (1999) Investigation of dominating factors on flattening behavior of plasma sprayed ceramic particles. Surf Coat Technol 120:124–130

Tscheliessnig R, Zörnig M, Herzig EM, Lückerath K, Altrichter J, Kemter K et al (2012) Nano-coating protects biofunctional materials. Mater Today 15:394–404

Tsukamoto H (2010) Design against fracture of functionally graded thermal barrier coatings using transformation toughening. Mater Sci Eng A 527:3217–3226

Tyagi A, Walia R, Murtaza Q, Pandey SM, Tyagi PK, Bajaj B (2019a) A critical review of diamond like carbon coating for wear resistance applications. Int J Refract Metal Hard Mater 78:107–122

Tyagi A, Pandey SM, Walia R, Murtaza Q (2019b) Characterization and parametric optimization of tribological properties of Mo blend composite coating. Mater Res Express 6:086428

Uusitalo M, Vuoristo P, Mäntylä T (2002) High temperature corrosion of coatings and boiler steels in reducing chlorine-containing atmosphere. Surf Coat Technol 161:275–285

Valette C, Devismes M-F, Voytovych R, Eustathopoulos N (2005) Interfacial reactions in alumina/CuAgTi braze/CuNi system. Scr Mater 52:1–6

Vignesh S, Shanmugam K, Balasubramanian V, Sridhar K (2017) Identifying the optimal HVOF spray parameters to attain minimum porosity and maximum hardness in iron based amorphous metallic coatings. Def Technol 13:101–110

Viscusi A, Astarita A, Gatta RD, Rubino F (2019) A perspective review on the bonding mechanisms in cold gas dynamic spray. Surf Eng 35:743–771

Viswanathan V, Katiyar NK, Goel G, Matthews A, Goel S (2021) Role of thermal spray in combating climate change. Emerg Mater 4:1–15

Voytovych R, Robaut F, Eustathopoulos N (2006) The relation between wetting and interfacial chemistry in the CuAgTi/alumina system. Acta Mater 54:2205–2214

Wagner N (2021) Effect of process parameters on twin wire arc sprayed steel coatings. J Mater Eng Perform 30:6650–6655

Wang J, Sun J, Zhang H, Dong S, Jiang J, Deng L et al (2018) Effect of spraying power on microstructure and property of nanostructured YSZ thermal barrier coatings. J Alloys Compd 730:471–482

Wang Q, Li Q, Zhang L, Chen DX, Jin H, Li JD et al (2022) Microstructure and properties of Ni-WC gradient composite coating prepared by laser cladding. Ceram Int 48:7905–7917

Winkless L (2015) Graphene coatings make steel corrosion-resistant. Elsevier

Winn AJ, Derby B, Webster JR, Holt S (2004) In situ characterization of interfaces between liquid tin–vanadium alloys and alumina by neutron reflection spectroscopy. J Am Ceram Soc 87:279–285

Xanthopoulou G, Marinou A, Vekinis G, Lekatou A, Vardavoulias M (2014) Ni-Al and NiO-Al composite coatings by combustion-assisted flame spraying. Coatings 4:231–252

Yao S-W, Li C-J, Tian J-J, Yang G-J, Li C-X (2016) Conditions and mechanisms for the bonding of a molten ceramic droplet to a substrate after high-speed impact. Acta Mater 119:9–25

Yin L, Murray BT, Singler TJ (2006) Dissolutive wetting in the Bi–Sn system. Acta Mater 54:3561–3574

Yin L, Chauhan A, Singler TJ (2008) Reactive wetting in metal/metal systems: dissolutive versus compound-forming systems. Mater Sci Eng A 495:80–89

Zhang C, Zhou H, Liu L (2014) Laminar Fe-based amorphous composite coatings with enhanced bonding strength and impact resistance. Acta Mater 72:239–251

Zhang Y, Hyland M, Tran AT, Matthews S (2016a) Effect of substrates temperatures on the spreading behavior of plasma-sprayed Ni and Ni-20 wt% Cr splats. J Therm Spray TechnOl 25:71–81

Zhang S, Wu J, Qi W, Wang J (2016b) Effect of porosity defects on the long-term corrosion behaviour of Fe-based amorphous alloy coated mild steel. Corros Sci 110:57–70

Zhang L, He T, Bai Y, Yu F-L, Fan W, Ma Y-S et al (2019) Velocity and temperature of in-flight particles and its significance in determining the microstructure and mechanical properties of TBCs. Acta Metall Sin (english Letters) 32:1269–1280

Zhang H, Wang S, Yang X, Hao S, Chen Y, Li H et al (2021) Interfacial characteristic and microstructure of Fe-based amorphous coating on magnesium alloy. Surf Coat Technol 425:127659

Zhong C, Liu F, Wu Y, Le J, Liu L, He M et al (2012) Protective diffusion coatings on magnesium alloys: a review of recent developments. J Alloy Compd 520:11–21